



# Predicting Solar Energetic Particles: Solar Storm Watch - Preparing for Space Odyssey

Athanasiос Papaioannou<sup>1</sup> · Roelf Du Toit Strauss<sup>2</sup> · David Lario<sup>3</sup> ·  
Rami Vainio<sup>4</sup> · Nicolas Wijesen<sup>5</sup> · Alexander Afanasiev<sup>4</sup> ·  
Anastasiос Anastasiadis<sup>1</sup> · Athanasiос Kouloumvakos<sup>6</sup>

Received: 10 September 2024 / Accepted: 10 August 2025  
© The Author(s) 2025

## Abstract

Space Weather effects produced by Solar Energetic Particles (SEPs) present a direct radiation hazard to crew and spacecraft equipment, first in interplanetary space, and then, due to secondary effects, within the Earth's magnetosphere and atmosphere. Being able to predict and/or forecast SEP events is of particular importance for the near-future planned manned missions to the Moon and Mars, as well as for our unimpeded daily living. In this review, we present key findings that have been utilized and/or explored by the scientific community over the last few decades to establish prediction schemes of SEP events. We first discuss empirical models where parameters related to the parent solar events (i.e. solar flares and coronal mass ejections) can be used to estimate both the probability of occurrence and critical properties (i.e. peak proton flux and/or fluence) of SEP events in the near-Earth environment and beyond. Next, we review physics-based modeling efforts of SEP events that are geared towards operational prediction, particularly focusing on SEP transport effects and multi-spacecraft observations. We furthermore explore the applicability of higher order multivariate, machine learning, and artificial intelligence methods and highlight the particular value and limitations of such advances. Finally, the most current operational approaches in the prediction of SEP events, together with future challenges that need to be addressed by the scientific community, are presented and discussed.

**Keywords** Sun: particle emission · Sun: solar flare · Sun: coronal mass ejections · Solar-terrestrial relations · Space weather

---

✉ A. Papaioannou

<sup>1</sup> IAASARS, National Observatory of Athens, GR-15236 Penteli, Greece

<sup>2</sup> Center for Space Research, North-West University, Potchefstroom, South Africa

<sup>3</sup> NASA, Goddard Space Flight Center, Heliophysics Science Division, Greenbelt, MD 20771, USA

<sup>4</sup> Department of Physics and Astronomy, University of Turku, FI-20500 Turku, Finland

<sup>5</sup> Centre for mathematical Plasma-Astrophysics, KU Leuven, B-3001 Leuven, Belgium

<sup>6</sup> The Johns Hopkins University Applied Physics Laboratory, Laurel, MD 20723, USA

## 1 Introduction

Solar Energetic Particles (SEPs) are protons, electrons and heavy ions that originate in association with eruptive solar phenomena at the Sun. Their energies range from tens of keV to several GeV. SEP events are energetic particle intensity enhancements observed by spacecraft in either the interplanetary (IP) space or even within the magnetosphere (for example at  $6.6 R_E$  by the Geostationary Operational Environmental Satellites, GOES) (see e.g. Anastasiadis et al. 2019) (see Fig. 1 for an overview). SEP events are primarily generated by two types of solar phenomena: solar flares and coronal mass ejections (CMEs). Solar flares result from the sudden release of magnetic energy in the Sun's atmosphere and accelerate particles through magnetic reconnection and associated shocks. CMEs, on the other hand, are large-scale eruptions of plasma and magnetic fields that are capable of driving shock waves in the solar corona and IP space, providing a more widespread and efficient mechanism for particle acceleration (Reames 2021).

A subset of SEP events, known as Ground Level Enhancements (GLEs), consists of extremely high-energy particles that penetrate Earth's atmosphere, producing secondary particle cascades detectable by ground-based neutron monitors (see Shea and Smart 2012; Bruno et al. 2018; Papaioannou 2023, and references therein). Major SEP events are typically associated with intense solar flares (i.e. usually  $>$  M-class or X-class), fast and wide CMEs, and specific solar radio bursts, such as type II radio bursts from shock formation and type III radio bursts from electron acceleration (Cane et al. 2010; Papaioannou et al. 2016).

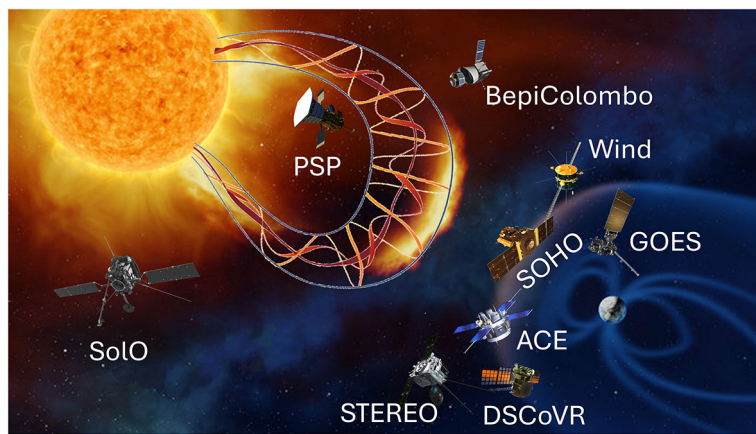


**Fig. 1** A schematic of geospace and the inner heliosphere, for context. An eruptive Sun and the interplanetary counterparts of a CME are denoted in the figure. The ICME is presented as a typical flux-rope, adapted from Akiyama et al. (2020). Missions presented span from distances very close to the Sun (i.e. the current missions of Solar Orbiter (Solo), Parker Solar Probe (PSP) & BepiColombo) to 1 AU (STEREO, GOES) and to L1 watchdogs (SOHO, ACE, Wind and DSCOVR). © AAS, ESA. Reproduced with permission

Space weather effects associated with SEPs include disruptions in communications, navigation, spacecraft electronics, power systems (Iucci et al. 2005), space missions (Cucinotta et al. 2001, 2002, 2008), and commercial aviation (see e.g. Tobiska et al. 2015; Beck et al. 2018; Matthiä et al. 2018; Bain et al. 2023). As technology reliance grows (see e.g. Vourlidas et al. 2023) and manned missions expand the development of a reliable scheme to provide

advanced warning of SEP events and their expected characteristics is essential. Human exploration plans transcend Earth's boundaries, aiming to venture deeper into the cosmos. Projects such as the Artemis mission (Creech et al. 2022) and the Moon village initiative (Woerner et al. 2016) carry potential risks for astronauts safety. As a result, a Space Odyssey embodies the integration of the vision, innovation, and scientific research, which is needed in order to place astronauts in orbit, land on the Moon, and plan missions to Mars. It emphasizes the importance of preparedness, such as predicting solar storms (i.e. SEP events), to ensure the safety and success of these daring ventures. In particular, it is of paramount importance to predict when and where an SEP event will (or will not) occur, what the maximum peak intensity of the event will be, and what the duration and ultimately the time profile of the SEP event will be. All these pieces of information are difficult to accurately predict due to the inherent complexity of the multiple physics processes involved in the development of the SEP events, from acceleration (near the Sun and in IP space) to the transport of SEPs towards Earth and beyond, producing large variability of SEP event properties, and leading to the current (relatively wide) gap in our knowledge. The specific mechanisms driving particle acceleration in association with solar flares and CMEs, such as the relative contributions of magnetic reconnection, shock acceleration, and turbulence, remain poorly understood (Vlahos et al. 2019). Similarly, the propagation of SEPs through the corona and within the heliosphere is influenced by factors like the magnetic field configuration of the corona and the IP space, the actual state of the solar wind medium where SEPs propagate and particle-wave interactions occurring during their transport, the mobility and evolution of the particle sources, making it challenging to model their arrival times and intensities (Strauss and Effenberger 2017). SEPs also exhibit significant spatial and temporal variability in intensity, duration, and energy spectra, which complicates accurate space weather forecasting (Reames 2023). Finally, predictive modeling is hindered by the complexities of these processes and the limited observational data available, underscoring the need for multi-point observations and advanced theoretical frameworks (Whitman et al. 2023). Bridging these gaps is essential for enhancing our understanding of SEP events and mitigating their impacts on space-based and terrestrial systems.

After more than 50 years of spacecraft observations, the consensus is that SEPs gain their energy in acceleration processes associated with the occurrence of solar flares and CMEs (Reames 1999, 2021; Papaioannou et al. 2016; Vlahos et al. 2019). SEP events are commonly classified as impulsive and gradual. Impulsive events are short in duration ( $\leq 1$  day), of low intensity and frequently observed, often in association with magnetic reconnection processes in coronal jets and solar flares. Gradual events, in contrast, last longer (up to several days), are less frequent than impulsive SEP events, and exhibit a wide range of intensities, spanning many orders of magnitude, typically associated with shock waves driven by large and fast CMEs (see e.g. Reames 1999, 2021). The transport of SEPs from their source to a given spacecraft is governed by the propagation conditions experienced in the corona and IP space (Kahler et al. 1999; Kahler and Vourlidas 2013; Lario and Karelitz 2014). The processes of particle acceleration may depend on the properties of their sources (coronal jets, CMEs, CME-driven shocks), and the presence of seed particles (the pool of (non)thermal or low energy particles from which a small fraction will be accelerated to high energy to become SEPs) (Tylka et al. 2005; Desai et al. 2006; Mewaldt et al. 2007), as well as, the possible interaction of multiple CMEs or shocks (Gopalswamy et al. 2002). Therefore, complex environmental and physical processes dominate the origin, acceleration, injection, and transport of particles in IP space, hindering the direct connection between the properties of SEP events and their progenitors at or near the Sun.

A temporal scale of at least four orders of magnitude adds to the difficulty of SEP prediction efforts (see details in Georgoulis et al. 2024). From the time when a solar flare occurs

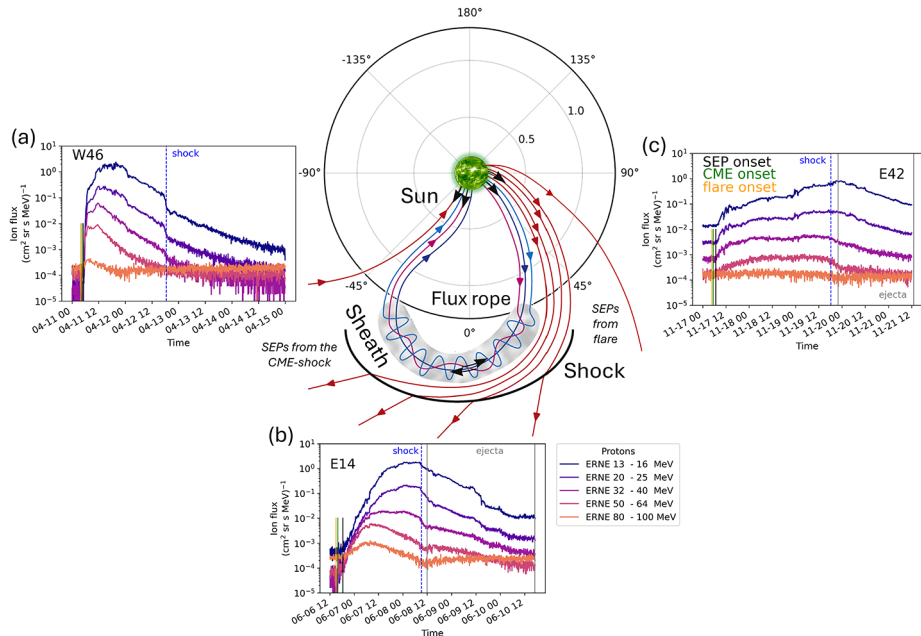


**Fig. 2** A schematic of the differences in the SEP intensity-time profiles that are ordered by varying connection to the parent solar eruptive events and the evolving CME-driven shock, originally proposed by Cane et al. (1988). Data from SOHO/ERNE spanning from 13–100 MeV have been used for the SEP events. These are: (a) 11 April 2000 W46°; (b) 06 June 2000 E14° and (c) 17 November 2001 E42°. The blue vertical solid lines within each SEP event denotes the crossing of an IP shock [<https://ipshocks.fi>]. The vertical short black (green) [orange] lines depict the SEP (CME) [flare] onset time per case. The event originating from a source near the central meridian (E14°) and eastern on E42° further incorporates the duration of the ejecta/magnetic cloud, which is taken from the Richardson & Cane ICME list available at: <https://izw1.caltech.edu/ACE/ASC/DATA/level3/icmetable2.htm> (Richardson and Cane 2024). The inner heliosphere was created using Solar-MACH (Gieseler et al. 2023). On top of this, a cartoon of an expanding interplanetary CME (ICME) adapted from Owens (2016) has been added. © AAS. Reproduced with permission

on the Sun ( $t_0$ ), the first photons arrive at Earth in  $\sim 8.33$  min, followed by the first energetic particles (assumed to be accelerated near the flare site) several tens of minutes after the flare. Then, a few tens of minutes later, the (assumed) CME-driven shock-accelerated particles arrive, followed by re-accelerated particles that are in space to continuously feed the interplanetary magnetic field (IMF) lines for hours as the CME expands and its driving shock propagates in the IP medium. Later, after a few days, the driving shock and the interplanetary counterparts of the initial CME may arrive at and pass by the observer leading to a final spike-like brief particle intensity enhancement – especially in lower energies, the so-called Energetic Storm Particle (ESP) events (Bryant et al. 1962) that occasionally may extend to high energies (Lario and Decker 2002; Cohen 2006; Lario et al. 2023, and references therein). The majority of ESP events are detected when CME-driven shocks originate near the solar central meridian (see e.g. Cohen 2006; Ameri et al. 2023, and references therein). These events are commonly accompanied by signatures of magnetized ejecta. ESP events may also be observed at the flanks of shocks associated with CMEs originating far east or west of central meridian but in contrast, these shock flanks are generally not followed by ICME-like structures (Santa Fe Dueñas et al. 2022). See details in Fig. 2.

Beyond the challenges posed by the temporal scale issue, the difficulty of predicting SEPs is further compounded by the variation in SEP time profiles depending on the observer's location (see e.g. Cane et al. 1988). Figure 2 illustrates the differences in SEP time profiles recorded by SOHO/ERNE for energies ranging from 13 to 100 MeV, utilizing SEP events from the catalogue by Paassilta et al. (2018). For the eastern event ( $E42^\circ$ ), the observer is poorly connected to the driving solar eruption, resulting in a gradual SEP rise. In this case, the lower-energy peak appears near the shock flank passage (marked by the blue vertical line). Here, the interplanetary CME impacts the observer, facilitating the identification of both the shock passage and the magnetized ejecta/cloud. This is evident in Fig. 2, where the ejecta passage is marked by two gray vertical lines. Conversely, for the SEP event linked to a near-central meridian eruption ( $E14^\circ$ ), the SEP time profile exhibits a relatively prompt rise, with the lower-energy peak occurring near the shock passage (also marked by a blue vertical line). Again in this case the interplanetary counterparts of the CME directly impact the observer and are similarly denoted in the plot (Papaioannou et al. 2020). In the case of the SEP event driven by a western solar eruption ( $W46^\circ$ ), the observer is magnetically well-connected to the solar event, leading to a distinct and prompt SEP increase across all energies. The SEP peak occurs rapidly, followed by a decay phase, and in this geometry, the observer may also encounter the shock flank. For all three illustrative SEP events in Fig. 2, the onset times of the SEP, CME, and flare events are marked by the black, green and orange short vertical lines, respectively. Thereby, a detail representation of the SEP time profile in advance of time is rather challenging and depends on several different factors.

Since the first observations of SEPs were possibly related to solar flares by Forbush (1946), based on a few decades of available measurements, associations between parent solar eruptions and SEP events have been firmly established (see e.g. Papaioannou et al. 2016; Richardson et al. 2017; Rotti et al. 2022b) and standard SEP lists at NOAA<sup>1</sup> and CDAW<sup>2</sup> are being regularly updated. As a consequence, several dependencies between the properties of the solar eruptions and SEP events have been identified. In the case of SEP events that have clear onset times and large intensity enhancements reaching several orders of magnitude, the association with parent solar events is usually well defined (see e.g. Klein and Dalla 2017). Many of these statistical correlations can be then directly applied to predict certain SEP event features. Nevertheless, despite the wealth of statistical and modeling studies, further improvement in our understanding of the science related to the acceleration and transport of SEPs is necessary in order to assess and predict SEP events.

## 2 Key Dependencies

A fairly reasonable correlation between the peak intensity of the SEP event and the speed of the CME has been identified (see e.g. Kahler et al. 1984; Kahler 2001; Gopalswamy et al. 2004; Cane et al. 2010; Rouillard et al. 2012; Richardson et al. 2014b; Kahler and Vourlidas 2014; Lario and Karelitz 2014; Papaioannou et al. 2016; Paassilta et al. 2017). Consequently, it has been established that fast and wide CMEs create favorable conditions for the acceleration of particles that result in large gradual SEP events since these are a prerequisite for establishing a shock, driven by the corresponding CME, able to efficiently accelerate particles as it propagates through the corona and IP space (see e.g. Kouloumvakos et al. 2019). This is expected since models of particle acceleration at CME-driven shocks

<sup>1</sup><https://umbra.nascom.nasa.gov/SEP/>.

<sup>2</sup>[https://cdaw.gsfc.nasa.gov/CME\\_list/sepe/](https://cdaw.gsfc.nasa.gov/CME_list/sepe/).

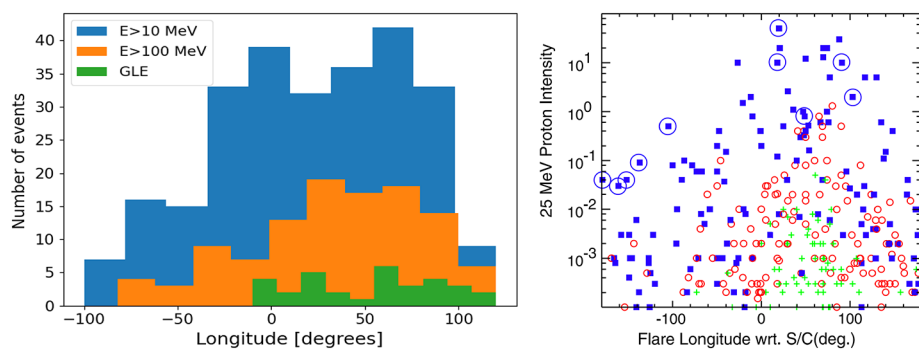


**Fig. 3** Distribution of SEP events, observed at Earth, as a function of the longitude of their parent flare (panel on the left hand side). The blue bars correspond to  $E > 10$  MeV SEPs, the orange bars to  $E > 100$  MeV and the green histogram to GLEs (panel on the left-hand side; created from data from Papaioannou et al. 2016). The peak intensities of  $\sim 25$  MeV proton events are plotted against the solar event longitude relative to the observing spacecraft for events from December 2009 to December 2013, when STEREO spacecraft were separated by more than  $58^\circ$  (panel on the right hand side). Symbols indicate detection at one (green cross), two (red circle), or three (blue square) spacecraft, with a point plotted for each observer in multi-spacecraft events (reproduced with permission from Richardson et al. 2014a, copyright by Springer)

point to a dependence of the acceleration rate on the shock speed in the solar wind frame (see Lee et al. 2012; Kouloumvakos et al. 2019). However, SEP intensity depends on multiple factors beyond the shock speed (see e.g. Lario and Karelitz 2014; Kouloumvakos et al. 2019). For example the shock strength, shock geometry, the presence of seed particles and the formation of waves upstream of the shock can affect the efficiency of the shock as a particle accelerator (see Tylka et al. 2005).

It is well known that the observation of a SEP event depends on the heliolongitude of the parent solar eruption and the evolution of the CME-driven shock (see Fig. 2) (e.g. Cane et al. 1988; Shea and Smart 1990, 1996; Belov et al. 2005; Cane et al. 2010; Paassilta et al. 2018). The arrival of SEPs at a given spacecraft is facilitated when a good magnetic connection is established between the spacecraft and the site of the solar eruption, so that particles can be routed efficiently to the observer site (see details in Van Hollebeke et al. 1975; Cane et al. 1988). In other words, western locations on the solar disk have a higher potential to result in an SEP event observed near Earth, due to the curvature of the Archimedean spiral IMF (Desai and Giacalone 2016; Klein and Dalla 2017) as shown in Fig. 3 (panel on the left hand side). Such findings were already established in previous studies utilizing observations from e.g. the Helios mission in conjunction to IMP-8 (see for example Kallenrode et al. 1993; Cliver et al. 1995; Kallenrode 1996). SEP observations by the Solar Terrestrial Relations Observatory (STEREO) mission (Kaiser et al. 2008) showed that wide-spread SEP events are detected at locations broadly separated in longitude (Papaioannou et al. 2014; Richardson et al. 2014a) from the site of the parent flare and particles can spread even over almost  $360^\circ$  (Gómez-Herrero et al. 2015). The STEREO mission greatly enhanced our understanding of such widespread SEP events by using multi-spacecraft observations. The two STEREO spacecraft positioned at different locations in the solar system, together with near-Earth spacecraft, provided unique perspectives on how SEPs propagate across wide regions of space. Figure 3 (right panel) illustrates that large SEP events can originate from any location on the Sun. Notably, SEP events detected by only one observer (green crosses) tend to originate from the western hemisphere and are relatively weak in terms of peak flux, suggesting that optimal magnetic connectivity is essential for their detection. Events observed

by two spacecraft (red open circles) are generally stronger and extend over a broader range of longitudes. Meanwhile, the most intense events in the sample are those detected by three spacecraft (blue squares), which also constitute the majority of events observed from behind the east limb. For these multi-spacecraft SEP events, CME-driven shocks were a plausible explanation, since shocks may provide broad particle sources. The magnetic connection established between the spacecraft and the propagating CME-driven shock could be linked to the observed intensity-time profiles of the SEP events and the time delays in the onset times of the SEPs at each observing point within the heliosphere (Rouillard et al. 2012; Lario et al. 2013, 2016; Kouloumvakos et al. 2023). Nevertheless, some SEP events are even observed when no magnetic connection with the CME-driven shock is established (e.g. Lario et al. 2014, 2017). In addition, it has been shown that even impulsive SEP events can be widespread (Dresing et al. 2012; Wiedenbeck et al. 2013) with particles undergoing perpendicular transport processes, spreading across field lines due to small-scale turbulence, meandering of the IP field, and large-scale structures in the heliosphere (see e.g. Kelly et al. 2012; Tan et al. 2013). On the other hand, the variability of the IMF with the presence of stream interaction regions (SIRs), and transient solar wind structures (interplanetary CMEs - ICMEs) influence not only SEP propagation (Laitinen et al. 2023) but also the structure of CME-driven shocks as they propagate in IP space (Wijesen et al. 2023). Thus, SEPs maybe trapped or guided along these structures, altering their arrival times, intensities and distribution (Richardson and Cane 1996; Lario and Karelitz 2014; Rodríguez-García et al. 2025).

Since the 1950s, it has been recognized that radio emissions at frequencies ranging from hundreds of MHz to a few tens of kHz provide crucial insights into the acceleration and propagation of SEPs (see e.g. Klein 2021a). These emissions help track the location and timing of particle release from the corona into IP space (Agueda et al. 2014; Kouloumvakos et al. 2015). Transient solar radio emissions serve as indicators of electron acceleration, primarily to energies of tens of keVs. Different types of radio bursts are associated with distinct acceleration processes: type III bursts signal electron beams escaping along open magnetic field lines (Cane et al. 2002), type II bursts indicate electrons accelerated by shock waves, and type IV bursts are linked to electrons trapped in closed-loop structures (Cane and Stone 1984). Type III radio bursts are fast-drifting emissions caused by electron beams moving outward at relativistic speeds ( $\sim 0.1\text{--}0.5c$ ). These electrons excite Langmuir waves, which then convert into radio emissions at the local plasma frequency and its harmonic. As the electron beam propagates into lower-density regions, the emission rapidly drifts to lower frequencies, with a fast frequency drift rate ( $\sim 10\text{ MHz/s}$ ) due to the high beam velocity. These bursts offer precise timing of SEP release and escape from the corona to IP space, originating at decimetric wavelengths ( $\sim 1\text{ GHz}$ ) in the low corona and extending down to  $\sim 20\text{ kHz}$  near 1 AU, marking the arrival of these electrons (Vainio et al. 2013).

Type II radio bursts are linked to shock waves, often driven by CMEs (Kahler et al. 1978). Their presence confirms shock-accelerated electron populations. These bursts are slow-drifting emissions produced as shocks propagate through the corona and IP space. The shock-excited electrons generate Langmuir waves and radio emissions at the local plasma frequency and its harmonic. As the shock moves outward into lower-density regions, the emission gradually drifts to lower frequencies, with a slow frequency drift rate ( $\sim 0.1\text{ MHz/s}$ ), reflecting typical shock speeds of hundreds to thousands of km/s—much slower than type III burst sources. All these radio emissions are fundamental for establishing the link between eruptive solar processes and SEP events in IP space (for recent reviews, see Vourlidas et al. 2020; Klein 2021b). However, both type II and type III radio bursts are usually observed in association with SEP events and thus both play a decisive role in the discrimination of SEP occurrence but do not help to distinguish the contribution of particle

acceleration at either shocks or in magnetic reconnection processes leading to solar flares (Kouloumvakos et al. 2015). This means that some major SEP events may have a contribution from both flares and CME-driven shocks (see e.g. discussion in Cane et al. 2010; Papaioannou et al. 2016).

Recent years have witnessed the development of increasingly sophisticated forecasting models, including empirical schemes, physics-based transport frameworks, and advanced machine learning methods. Each approach provides unique insight into the SEP acceleration and transport problem, though none is yet sufficient in isolation. This diversity of modeling efforts reflects the complex, multi-physics nature of SEP events and the evolving demands of operational forecasting.

### 3 Predicting SEP Events

Observational dependencies such as those mentioned in Sect. 2 (e.g. Kahler and Ling 2015; Kahler et al. 2015) have been utilized as indicators/classifiers for the development and implementation of empirical SEP prediction concepts. However, the prediction of SEP events is offered on different time scales, directly driven by the input employed. There are long-term and short term predictions, with the former termed as forecasts and the latter as nowcasts (see details and definitions in Anastasiadis et al. 2019). The majority of the current operational concepts offer nowcasts, while the scientific community is making extensive efforts to develop accurate forecasts with increased lead time (see e.g., Falconer et al. 2011; Whitman et al. 2023; Georgoulis et al. 2024, and references there in). The nowcasting of SEP events aims to combine signatures of solar eruptive events and to utilize these (or any of their combinations thereof) as inputs to models (concepts), with the aim of increasing prediction accuracy (see e.g. Swalwell et al. 2017). Such efforts, exploiting flare and/or CME characteristics, have been proposed by the scientific community (see Whitman et al. 2023). In particular, below, we distinguish the concepts according to the solar phenomena used as input.

**Solar Flares** Initially (in the 1970s and 1980s), and to the present, flare characteristics were the main contributor to such SEP prediction concepts. Several reasons led to the use of flares: (a) flare properties are routinely delivered by GOES patrol measurements since 1976, (b) flare soft X-ray (SXR) observations are available shortly after their occurrence at a cadence of a few minutes (i.e. 1-min or 5-min) and thus perfectly suit operations, and (c) a wealth of observational evidence (see Sect. 2) pointed to their close association with the occurrence of SEP events (Garcia 1994a; Belov 2009). In addition, hard X-ray (HXR) signatures of flares have been used as indicators of SEPs (Garcia 1994b; Kiplinger 1995). Two early SEP nowcasting systems were developed by the National Oceanic Atmospheric Administration (NOAA) and the Air Force Research Laboratory (AFRL), namely PROTONS (Balch 1999) and the Proton Prediction System (PPS) (Kahler et al. 2017, and references therein). More recently, the UMASEP (see Fig. 4) model was developed using an existing lag correlation between the solar flare SXR flux and the near-Earth particle flux (either differential or integral). The UMASEP scheme was initially trained for  $E > 10$  MeV (Núñez 2011) and later extended to higher ( $E > 100$  MeV and  $E > 500$  MeV) proton energies (Núñez 2015; Núñez et al. 2017). Note that solar flares originating from active regions behind the east or west limbs of the Sun and associated with SEP events cannot be directly observed from Earth (i.e. by GOES) presenting an observational limit.

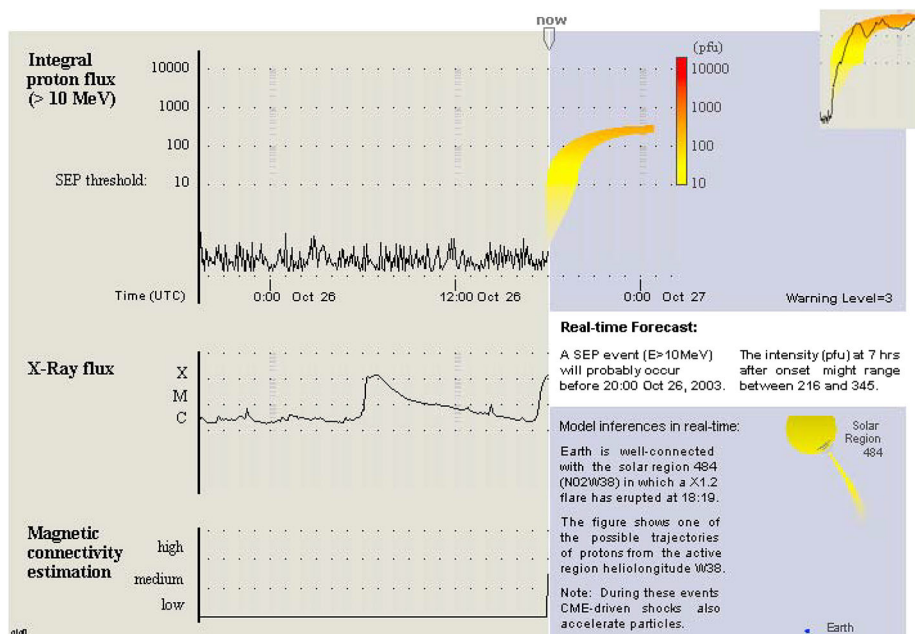


**Fig. 4** Illustration of the UMASEP graphical interface for the SEP event on 26 October 2003. The top panel provides the  $E > 10$  MeV proton measurements from GOES, while the middle panel depicts the GOES soft X-ray flux. The prediction is illustrated by the orange-yellow shading extending from the observed proton flux (black graph). The bottom panel refers to the magnetic connectivity of the flare to the observer (i.e. Earth). The small top right chart is not part of the forecaster output; it shows the comparison between the predicted integral proton flux and the subsequent observed evolution of the integral proton flux for this event, demonstrating that the forecast was successful. The bottom chart shows an illustration of a possible route of the solar protons from the corresponding heliolatitude towards the near-Earth environment. Reproduced with permission from Núñez (2011), copyright by AGU

**CMEs** Large intense gradual SEP events have direct space weather relevance (see Sect. 1) and therefore CME identifications have been explored by the scientific community (see Table 10 of Whitman et al. 2023). However, there are several challenges to using CME observations to trigger SEP predictions (Richardson et al. 2015). In particular: (a) CME data obtained from the Large Angle Spectroscopic Coronagraph (LASCO) on board SOHO have been made routinely available only since 1996; (b) the telemetry of the SOHO data imposes a limit on the data reception which creates a varying time delay between data reception and data retrieval depending on the time difference of the CME observations to data acquisition; (c) an additional delay that arises from manually extracting CME parameters after data reception, which could be minimized through automation and (d) however, automated methods for the extraction of CME characteristics may provide outputs with significant uncertainty and variability, especially for Earth-directed CMEs when only near-Earth coronagraph images are available (Robbrecht and Berghmans 2004) (CACTUS: Robbrecht and Berghmans 2004; SEEDS: Olmedo et al. 2008; CORIMP: Byrne 2015), and differences in CME parameters obtained using different methods in different catalogs and the real-time availability are demanding (see the relevant discussion in Papaioannou et al. 2025).

One recent approach is to derive simple 2D probability functions for the probability of SEP occurrence based on the width and speed of CMEs, as well as linear correlations between the SEP peak flux and CME speed (Papaioannou et al. 2018b) which were

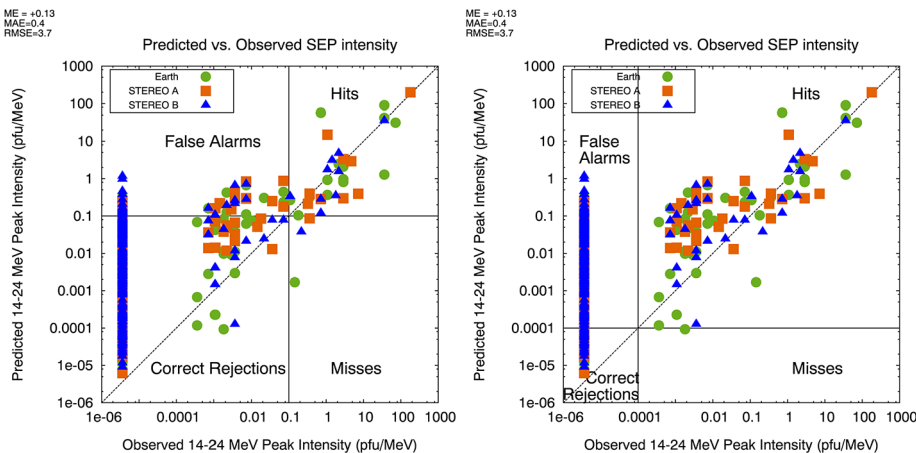


**Fig. 5** SEPSTER Predicted versus Observed peak proton intensities at  $E = 14 - 24$  MeV. Each color and shape corresponds to a different observer (i.e. Earth, STA, STB). The different plots serve as contingency tables showing the false alarms, hits, misses and correct rejections based on a threshold of 0.1 (panel on the left-hand side) or 0.0001 pfu/MeV (panel on the right-hand side) which is approximately the instrument's threshold (from Richardson et al. 2018)

then integrated into the FORcasting Solar Energetic Particle and Flares (FORSPEF) tool (Anastasiadis et al. 2017). Other approaches include SEPSTER (SEP predictions based on STEREO observations), that uses a formula providing the 14-24 MeV proton peak flux of SEP events observed by SOHO, STEREO-A and STEREO-B using as parameters the parent CME speed and the longitudinal angular distance between the site where the CME originated and the footpoint of the magnetic field line connecting the observing spacecraft on the Sun (Richardson et al. 2018). Figure 5 demonstrates the predicted SEP intensities from SEPSTER versus the observed ones for protons at 14-24 MeV. This concept was further expanded in order to provide the expected proton peak flux particle spectra ranging from 10-130 MeV at 1 AU (Bruno and Richardson 2021). SEP prediction using observations from coronagraphs such as LASCO (and STEREO COR2) is also limited by the need for the CME to have propagated above the inner limit of the field of view at  $\sim 2 R_S$ , by which time high-energy SEPs may already be arriving at 1 AU. In order to detect CMEs earlier, St. Cyr et al. (2017) proposed using CME observations from ground-based coronagraphs which have a field of view extending from close to  $1 R_S$  and a low data latency of the order of minutes, though suffer from a low duty cycle, requiring a world-wide chain of stations to provide 24 hour monitoring.

**Radio Bursts** Radio burst data from ground based sources<sup>3</sup> are available in near-real time mode. In addition, real-time observations from the SWAVES instrument (Bougeret et al. 2008) on STEREO A<sup>4</sup> have also been recently introduced, extending the real time radio observations down to lower frequencies and hence further from the Sun (see Posner et al. 2024). In addition, data from Wind/WAVES (Bougeret et al. 1995) are currently not made available to the scientific community in a near-real time. Nonetheless, a scheme based on

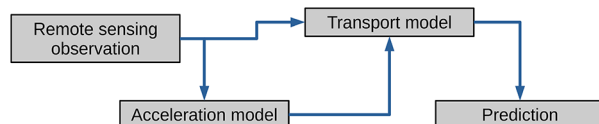
<sup>3</sup><https://www.e-callisto.org/index.html>, <https://secchirh.obspm.fr/>.

<sup>4</sup>[https://stereo-ssc.nascom.nasa.gov/beacon/beacon\\_in situ.shtml](https://stereo-ssc.nascom.nasa.gov/beacon/beacon_in situ.shtml).

type III radio bursts observations from Wind/WAVES called Empirical model for Solar Proton Events Real Time Alert (ESPERTA) was put forward by Laurenza et al. (2009). This scheme uses solar flare locations, SXR flare class, and time-integrated type III radio emission at  $\sim 1$  MHz as evidence of SEP release into IP space to predict SEP events. This concept was recently re-validated (Alberti et al. 2017), and further extended to the prediction of very strong radiation storms (Laurenza et al. 2018) with considerable success. Moreover, recently Laurenza et al. (2024) demonstrated the successful implementation of ground-based observations from LOFAR (LOw-Frequency ARray; van Haarlem et al. 2013) radio data into the ESPERTA concept. Furthermore, Richardson et al. (2018) demonstrated that observations of type III radio bursts could be used to identify CMEs with or without SEP events. As a result, there is a strong potential for incorporating radio burst data in SEP prediction, though the limited real-time observations especially at lower frequencies hampers the practical applicability of the concepts in real-world scenarios.

**In-Situ Particles** Posner (2007) demonstrated that near relativistic electron fluxes can be successfully used for nowcasting the arrival of 30–50 MeV protons. The Relativistic Electron Alert System for Exploration (REleASE) concept is based on a matrix that maps the registered electron intensity to the expected intensity of the protons and thus provides a deterministic nowcasting of the expected proton flux in each moment of time. The concept is based on the delay between electron and proton onsets, which ranges from 20–30 minutes up to 1 hour (Posner 2007). In addition, based on this delay and utilizing electron and proton intensities, most recently Stumpo et al. (2024) developed a machine learning algorithm for the prediction of proton SEPs (see details in Sect. 3.2). In-situ particle measurements from ground based detectors like neutron monitors have further been used for signaling the subsequent arrival of lower energy protons (i.e.  $E > 10$  MeV). This is also based on the fact that these near relativistic protons ( $E \geq 433$  MeV) travel between the Sun and Earth almost scatter free and reach Earth in just a few minutes. As a result, NMIs can be used as a warning for the arrival of lower energy protons, as this is recorded onboard satellites (see details in Kuwabara et al. 2006; Souvatzoglou et al. 2014, and references therein). One major observational gap is, however, the unavailability of reliable in-situ measurements of high-energy protons ( $E > 300$  MeV), even though those are of particular concern for space exploration (see details in Vourlidas et al. 2023).

**Fig. 6** A very simplified flow diagram of the typical SEP physics-based prediction model



### 3.1 SEP Acceleration and Transport

The scheme of a typical simplified physics-based model is outlined in Fig. 6. The model chain is usually initiated with some combination of remote-sensing observations, which feeds into an acceleration module or model. This acceleration model deals with the local acceleration of a seed particle population at the acceleration site, which can be the site of a solar flare or the front of a propagating shock. This accelerated population of SEPs are then introduced into an interplanetary model (or module) that simulates the transport of the SEPs

through IP space, resulting in a predicted SEP intensity at an observer position. Physics-based prediction models try to implement governing equations for each step in the SEP acceleration and transport process that capture the essential physical mechanisms and describe them, ideally, from first principles. This is a different approach from those used in empirical and machine learning models where statistical correlations between observed acceleration signatures (e.g. the flares class) and in-situ particle measurements (e.g. the peak SEP flux at a particular energy) are used without trying to necessarily understand the physical processes responsible for the coupling, although they may, of course, be causally connected and physically motivated and/or explained.

The rationale for separating the SEP acceleration and transport processes into distinct modules is because of the vast differences in their underlying length and time scales. That is, transport models are typically solved on scales of the order of fractions of an AU, and can therefore not resolve kinetic length scales, such as those in shocks or reconnecting field lines, where acceleration mechanisms take effect. However, the separation between transport and acceleration models introduces several complexities. For instance, the acceleration process at a CME-driven shock can happen across the entire shock front, which is characterized by varying local plasma and shock conditions, all of which influence the acceleration environment. These scales also change throughout the heliosphere as e.g. the particles' gyro-radius increases due to the magnetic field strength decreasing away from the Sun. Similarly, SEP transport is strongly influenced by the small-scale turbulence that can scatter SEPs, exhibiting considerable variability depending upon local solar wind conditions. Furthermore, certain regions pose challenges to the clear demarcation between transport and acceleration processes, such as the turbulent sheaths downstream of shock waves. In the remainder of this section, we provide an overview of some of the particle acceleration and transport mechanisms that shape SEP events.

### 3.1.1 Acceleration Mechanisms

The so-called “the solar flare myth” (Gosling 1993) led early investigators to associate SEP events exclusively with the occurrence of solar flares. The role of CME-driven shocks in gradual SEP events became later evident when analyzing intensity-time profiles of SEP events generated from different longitudes (Cane et al. 1988) as well as the observations of SEP events lacking a flare association (e.g. Sanahuja et al. 1983). Although the most intense and energetic SEP events are accompanied by intense type III emissions which might indicate a flare contribution to these SEP events (Cane et al. 2002), the role of flares in the acceleration of SEPs is still debatable (see Reames 2023, and references therein).

When studying the onset times of MeV electron and protons SEPs, Richardson et al. (2014a) found that if interplanetary transport is assumed to be independent of longitude, electrons and protons have to be accelerated by different sources expanding at different rates as electrons arrive before protons at all longitudes, and the electron and proton delays to onset increase as the magnetic connection becomes poorer. However, when *longitudinal* transport (i.e. cross-field diffusion) is included, the different arrival times can be explained by a single source (Strauss et al. 2023). The dominant acceleration process could potentially also be energy dependent: Strauss et al. (2017) have shown that near-relativistic ( $\sim 100$  keV) electron observations are consistent with acceleration at a compact source (usually at the site of the solar source), while at higher energies (i.e. of the order of MeV) Dresing et al. (2022) suggested that electrons could be associated with the processes of particle acceleration at CME-driven shocks.

Various particle acceleration mechanisms have been proposed to occur at shock waves, including diffusive shock acceleration (DSA; e.g., Krymskii 1977; Bell 1978; Drury 1983)

and shock drift acceleration (SDA; e.g., Ball and Melrose 2001), among others (see Vainio and Afanasiev 2018, for an overview). These mechanisms typically depend on the gyro radius and frequency of the particles, introducing thus a dependence on the energy, mass, and electrical charge of the particles. Additionally, local shock properties are expected to play a significant role. For example, the effect of the shock's obliquity on particle acceleration has been clearly established at Earth's bow shock (e.g., Eastwood et al. 2005), and correlations between the shock's Mach number and SEP intensities have been observed (e.g., Kouloumavakos et al. 2019; Dresing et al. 2022). Adding to the complexity, these shock properties can significantly vary due to the presence of upstream solar wind streams with differing speed and density (e.g., Wijzen et al. 2023), as well as due to the presence of turbulence in the upstream plasma (e.g., Trott et al. 2023).

Moreover, shock-accelerated particles propagating in the shock vicinity may amplify the ambient turbulence encountered upstream of the shock (i.e. the so-called self-generated turbulence) (Bell 1978). The analytical theory of SEP acceleration in shocks self-consistently accounting for self-generated (Alfvénic) turbulence was elaborated in a number of studies (e.g., Lee 1983, 2005; Vainio 2003), which was followed by the development of several simulation models (e.g., Ng et al. 2003; Ng and Reames 2008; Vainio et al. 2007; Vainio and Laitinen 2008; Afanasiev et al. 2015). The SOLar Particle Acceleration in Coronal Shocks (SOLPACS) model (Afanasiev et al. 2015) has demonstrated a very good agreement when comparing simulated proton distributions and wave intensity spectra in the shock upstream region with those obtained from the observations from STEREO and Solar Orbiter (Afanasiev et al. 2023; Nyberg et al. 2024) (Fig. 7).

Once particles escape their acceleration site, they propagate through the solar wind where they undergo scattering processes, as described in the subsequent section. This scattering can significantly modify the shape of the SEP intensity time profiles, energy spectra and particle anisotropies, as evidenced by observations near Earth (Strauss et al. 2020). Spacecraft observations closer to the Sun (such as PSP, BepiColombo, and Solo), very near or directly at the presumed acceleration region, provide valuable insights, as they can sample SEPs before they undergo significant alteration during propagation through the turbulent interplanetary medium.

### 3.1.2 Transport Mechanisms

Particles undergo various deterministic and stochastic processes while propagating through the turbulent solar wind. Due to the diverging interplanetary magnetic field away from the Sun, and the fact that the magnetic moment of the particles are conserved in a relatively smooth magnetic field, the pitch-angle of the particles decreases as they propagate away from the Sun into IP space. This effect, termed *focusing*, leads to the formation of SEP beams focused along the IMF lines and explains why SEP events are often highly anisotropic, especially at the onset of the events. The magnetic focusing is, however, counteracted by interactions between the SEPs and turbulent magnetic fluctuations that scatter their pitch-angle in a stochastic fashion. These scattering processes break the conservation of the magnetic moment and, from the perspective of an SEP distribution, give rise to *pitch-angle diffusion*. As a consequence, in situ observations show that an SEP event tends to become more isotropic as the event progresses. Pitch-angle diffusion and focusing are two examples of magnetic field aligned processes that modify the SEP distributions as they move away from the Sun. Additional processes, such as perpendicular diffusion (again a stochastic process), field line random walking (a stochastic meandering of magnetic field lines), and/or drift effects (a deterministic process), may lead to cross-field transport where SEPs detach from their original magnetic field lines and move to adjacent field lines originally not connected to the source.

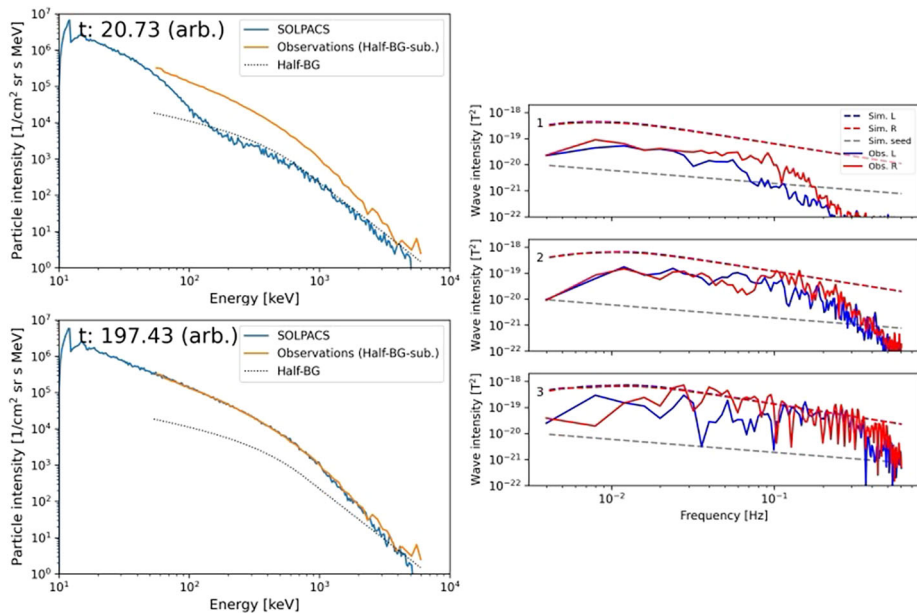


**Fig. 7** Left: Comparison of the proton energy spectra at the shock as resulting from SOLPACS simulations (blue line) versus the spectrum obtained from Solar Orbiter particle data (orange line) in the October 30, 2021 ESP event at an intermediate simulation time (upper plot) and in the steady state (bottom plot). Right: Comparison of the simulated Alfvén wave spectra (red and blue dashed lines) with the wave spectra obtained from Solar Orbiter magnetic field measurements (solid lines) in the upstream region at three different distances from the shock. It illustrates the wave intensity of left- (L) and right-handed (R) polarization modes as a function of wave frequency for a two-component injection SOLPACS case (dashed colored lines). It also presents the seed wave population of SOLPACS (gray dashed line) and the fast Fourier transform (FFT) wave spectra derived from Solar Orbiter/MAG observations (solid colored lines). Assembled from and details in Nyberg et al. (2024)

In the most basic formulation, the evolution of the SEP distribution function,  $f$ , is governed by a transport equation of the form (Skilling 1975; van den Berg et al. 2020)

$$\frac{\partial f}{\partial t} + \nabla \cdot (\vec{v}_{\text{gc}} f) + \frac{\partial}{\partial \mu} \left( \frac{1 - \mu^2}{2L} v f \right) = \frac{\partial}{\partial \mu} \left( D_{\mu\mu} \frac{\partial f}{\partial \mu} \right) + \nabla \cdot (\mathbf{D}_{\perp} \cdot \nabla f)$$

The left-hand side of this equation represents deterministic processes that govern SEP transport. These include particle streaming along the average magnetic field line direction (described by the pitch-angle focusing term), gradient and curvature drifts (captured in the guiding center velocity,  $\vec{v}_{\text{gc}}$ ), and convection with the solar wind, which moves radially outward. These terms describe how SEPs systematically evolve through the heliosphere due to the large-scale structure and flow of the interplanetary magnetic field and solar wind (Dalla et al. 2013; van den Berg et al. 2021), where the guiding center velocity can be expressed as:

$$\vec{v}_{\text{gc}} = v_{||} \hat{b} + \vec{v}_{\text{drift}} + \vec{v}_{\text{convection}} + \dots \quad (1)$$

where  $\hat{b}$  indicates the direction of the average magnetic field, and particle focusing determined by the focusing length,  $L$ , which is determined by the structure of the global magnetic

field. Stochastic (i.e. diffusive) processes are included in the right-hand side of Eq. (1), including pitch-angle diffusion, quantified by the pitch-angle diffusion coefficient  $D_{\mu\mu}$ , and perpendicular diffusion, quantified by the perpendicular diffusion tensor  $\mathbf{D}_{\perp}$ . Note that we generally do not work with the pitch-angle itself, but rather the cosine of the pitch-angle  $\mu$ . Additional processes can be included into the transport equation, including adiabatic energy losses, although these can mostly be considered negligible when considering the transport of near-relativistic SEPs between the Sun and Earth (Ruffolo 1995). Nevertheless, this process can be employed to simulate the DSA process (e.g., Wijsen et al. 2019).

After solving the transport equation to obtain  $f$ , the corresponding omnidirectional intensity can be calculated by averaging over pitch-angle. This omnidirectional intensity is the operational quantity most frequently compared to spacecraft measurements. Additionally, the associated first-order parallel anisotropy,  $A$ , can be calculated as:

$$A = 3 \frac{\int_{-1}^{+1} \mu f(\mu, z, t) d\mu}{\int_{-1}^{+1} f(\mu, z, t) d\mu}, \quad (2)$$

where  $A = 0$  (indicating an isotropic distribution of particles) and  $A = \pm 3$  (indicating a beam of particles propagating parallel (+) or anti-parallel (−) to the IMF). Anisotropy serves as a valuable indicator for determining the arrival direction of particles, allowing inferences about whether SEPs propagate along magnetic field lines, undergo significant scattering processes, or propagate across the magnetic field direction (Sanderson et al. 1985; Lario et al. 2004; Dresing et al. 2012; Brüdern et al. 2022). Unfortunately, most current three-axis stabilized spacecraft carrying remote-sensing observing instrumentation provide limited anisotropy measurement, requiring several telescopes with different FOVs.

While the deterministic processes can be calculated directly from the global magnetic field (whether a global Parker IMF or a numerically calculated background field obtained from MHD models), the diffusion coefficients  $D_{\mu\mu}$  and  $\mathbf{D}_{\perp}$  should, in principle, be calculated from first principles using an appropriate theory and observations of the embedded magnetic field turbulence. However, the magnetic field cannot be measured throughout all the trajectory followed by the particles, and some assumptions on how turbulence evolve with heliocentric distance are required and its translation to the effects produced into the SEP transport is very challenging and complex (Strauss and le Roux 2019). Additionally, the role of perpendicular diffusion in spreading SEPs in the inner heliosphere is still being debated by the community (Dröge et al. 2014, 2016; Dresing et al. 2023)

The pitch angle scattering processes undergone by the particles is often parametrized by the parallel mean free path,  $\lambda_{\parallel}$ . An isotropic perpendicular diffusion coefficient,  $\kappa_{\perp}$ , can be calculated by averaging the pitch-angle dependent perpendicular diffusion coefficient over pitch-angle. This quantity is again related to the perpendicular mean-free-path by  $\lambda_{\perp} = 3\kappa_{\perp}/v$  (Shalchi 2009; Strauss and Fichtner 2014). While many earlier studies neglected the effect of perpendicular diffusion, more recent simulation work by e.g. Zhang et al. (2009, 2023) and Dröge et al. (2010, 2014) have shown the necessity to include this transport process to explain multi-spacecraft SEP observations. It is now common for SEP transport models to include perpendicular diffusion. However, not all physics-based SEP forecasting models have incorporated this process, mostly due to the added level of complexity introduced and the need of using an additional unconstrained parameter.

### 3.1.3 Model Complexity and Feasibility

While Fig. 6 present a simplified view of a SEP prediction model, a more realistic, and therefore much more complex sketch of a physics-based model is presented in Fig. 8. Here, differ-

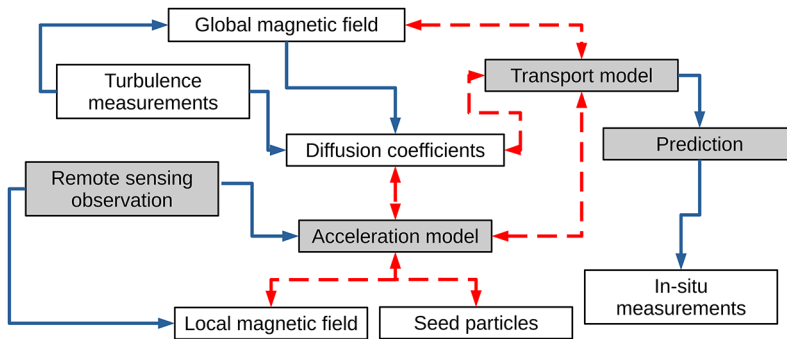
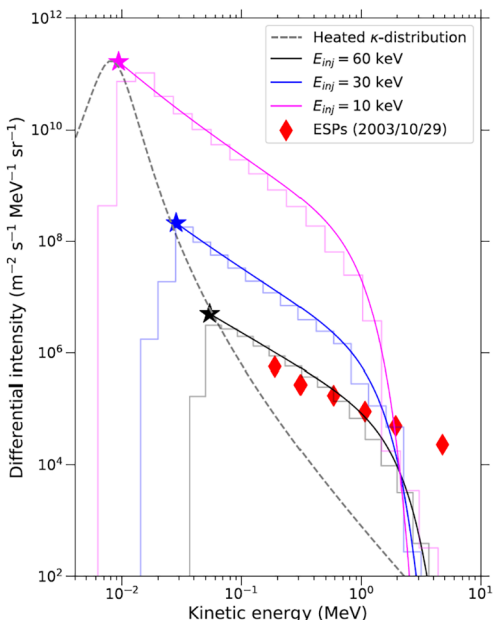


**Fig. 8** Possible complexities of a physics-based SEP prediction model. Compared to Fig. 6, white boxes now indicate additional quantities and/or processes that may need to be taken into account to correctly describe ‘realistic’ SEP transport. Blue lines illustrate the usual (one way) flow of information that feed into components of the model, while red lines show potential forward- and back-reactions that may have to be included for consistency. An example of this is output from the transport model, i.e. the calculated time-dependent SEP distribution, that could lead to wave-amplification by the streaming SEPs. This amplification will enhance the background turbulence, which will in turn change the magnitude of the diffusion coefficients, that will feed into the transport model. Similarly, both the amplified waves and the particles themselves, if they contain sufficient pressure, might modify the local plasma environment and therefore also the global (large scale) magnetic field. Again this feeds into the transport model creating a second feedback loop. Many such mechanisms can, in theory, be incorporated into a physics-based model, for e.g. the streaming SEPs losing energy by forming Langmuir waves that decay into radio waves that form radio bursts, ultimately leading to an incredibly complex and non-linear model that can currently, in practice, not be solved due to both computational constraints but also the lack of in-situ measurements

ent observations and parameters are needed to feed into an acceleration model. These include details of the local magnetic structure and seed particle population in the solar corona and throughout IP space, which are often not directly measurable. Similarly, details of the local turbulence conditions directly at the acceleration site has to be specified, while the accelerated particles, streaming away from the acceleration site, can themselves modify the local turbulence and therefore the diffusion coefficients governing their transport. The (probably numerical) acceleration model then feeds into a (again numerical) transport model that propagates the accelerated particles through the heliosphere until a SEP prediction can be made at a given heliospheric location. For past events, the model chain can be run with different initial conditions until a satisfactory comparison between model results and observational data is achieved. However, for an operational setting, the lack of actual observations of the inputs needed to run these models inhibits such a parameter study. The question is whether a physics-based model, as depicted in Fig. 8 is feasible at all. There are indeed possible technical constraints, such as the long run-times associated with all these numerical models. However, more concerning is the fact that current available observations do not provide all the required information to determine the variable inputs and parameters used in these models. For example, specific details on the seed particle populations, the local magnetic field structure, turbulent conditions, or the diffusion coefficients required to determine the output of the particle acceleration mechanisms assumed in these models are unknown. And we are not even certain about the contribution that different acceleration mechanisms might have in a SEP event.

Consider, for instance, the simulation results of Prinsloo et al. (2019) reproduced in Fig. 9. Here the dashed line shows the assumed energy dependence of the seed particle population (in this case a heated non-thermal distribution) which is then accelerated by a travelling interplanetary shock (different model runs shown by the purple, blue, and black

**Fig. 9** The results of Prinsloo et al. (2019) showing a non-thermal seed population undergoing DSA acceleration at a travelling interplanetary shock for different assumptions of the injection energy, resulting in vastly different energy spectra. © AAS. Reproduced with permission



curves) and compared to the resulting SEP observations indicated by the red symbols. While, in general, the seed particle distribution is not well known (i.e. for a thermal distribution the temperature at the acceleration site might not be known or cannot be derived from remote-sensing observations), these results illustrate a much more intricate problem: The different model results are for different assumptions of the so-called injection energy (Desai and Giacalone 2016) in the DSA mechanism with a certain set of parameters. That is, the minimum energy particle that can be re-accelerated during the DSA process. For these simulations, the injection energy is varied by a factor of 6, while the resulting particle spectra change by almost 6 orders of magnitude. The injection energy depends on the local turbulence conditions and transport coefficients, which cannot be sampled, but have an extremely large influence on the resulting SEP predictions. The selection of optimal parameters needs to be discussed and justified. While complex model chains have demonstrated success in reproducing historical SEP events, the necessity for ad-hoc adjustments to free parameters renders such models inadequate for operational purposes. To overcome these limitations and be practically feasible in an operational setting, different models are developed to simplify different aspects of the SEP acceleration and/or transport. Several examples of such models, with different levels of complexity and making a variety of different model assumptions, can be found in Whitman et al. (2023). Below, we highlight a few of the physics-based models that attempt to include as much physics as possible by incorporating theory elements (in either the acceleration and/or transport models) with different levels of complexity under different assumptions

An example of the current state-of-the-art physics-based SEP prediction models is PARADISE (PArticle Radiation Asset Directed at Interplanetary Space Exploration; Wijssen 2020). This model uses a magneto-hydrodynamic (MHD) simulation of the background heliospheric plasma and magnetic field, in this case EUFORIA (EUropean Heliospheric FORecasting Information Asset; Pomoell and Poedts 2018) and simulates the acceleration and transport of SEPs, in the test particle limit (e.g. without affecting the background

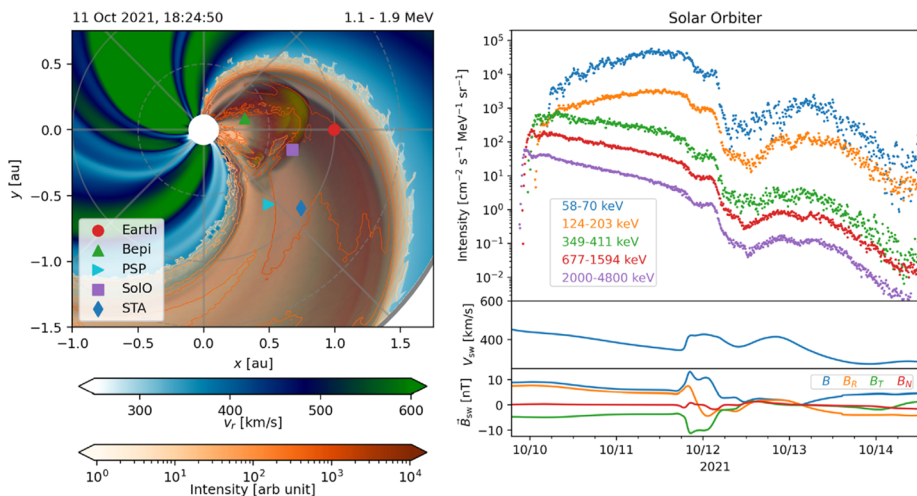


**Fig. 10** Example of results obtained from the coupled EUPHORIA and PARADISE model. The left panel shows the SEP distribution super-imposed on top of the MHD background while the right panel shows the resulting SEP temporal profile at different energies and solar wind parameters from the MHD model. This example is taken from Whitman et al. (2023)

plasma), within this MHD environment. This allows the model to capture the effect of the non-Parkerian (Parker 1958) solar wind conditions, e.g., due to the presence of preceding CMEs (Niemela et al. 2023) or solar wind streams of varying speed (Wijsen et al. 2023).

An example of this model's output is shown in Fig. 10. The coupled EUHFORIA+PARADISE model operates in a fully three-dimensional (3D) space, allowing for comprehensive simulations of SEP propagation. However, this 3D approach also demands extensive computational resources, making real-time predictions computationally expensive.

Furthermore, it is important to note that models like PARADISE do not capture several physical processes, as illustrated in Fig. 8. For instance, SEP transport is typically limited to a test particle approach, neglecting the back-reaction of the resulting particle distribution on the MHD background (such as particle pressure or wave excitation). Additionally, the seed particle population is typically prescribed as an ad-hoc particle distribution, and the exact transport coefficients (i.e., the parallel and perpendicular mean-free-paths) are treated as free parameters throughout the domain to simplify and speed up the computations.

As a step towards overcoming the mentioned limitations, a new modeling framework for forecasting SEP events, PARASOL, has been recently introduced (Afanasiev et al. 2025). In this framework, the turbulence amplification in the foreshock region is incorporated into PARADISE through a semi-analytical foreshock model obtained using self-consistent simulations of proton acceleration with SOLPACS. This approach allows including the self-consistent treatment of particle acceleration in shocks into the global 3D transport simulation model without a substantial increase in the computational cost. In contrast, the direct coupling of PARADISE and SOLPACS would result in a computationally heavy simulation model unlikely usable in the operational space-weather context.

Similar physics-based models are e.g. M-FLAMPA (Multiple-Field-Line-Advection Model for Particle Acceleration; Sokolov et al. 2004), iPATH (improved Particle Acceleration and Transport in the Heliosphere; Hu et al. 2017), that uses a 2D MHD background that has recently been upgraded to 3D (see e.g. Li et al. 2021), STAT (Solar Particle Event Threat Assessment Tool; Linker et al. 2019) that used a 3D MHD background, but only considers

1D SEP transport along magnetic field lines, and SOFIE (SOlar wind with FIELd lines and Energetic particles; Zhao et al. 2024), that utilizes the Alfvén Wave Solar-atmosphere Model Realtime (AWSOM-R) for the background solar wind, on top of which CMEs are launched as imbalanced magnetic flux ropes using the Eruptive Event Generator using Gibson-Low model (EEGGL). The acceleration and transport processes of SEPs are modeled by M-FLAMPA. SOFIE aims to tackle the free parameter problem by determining suitable default values through ensemble studies, spanning the model parameter space and/or by deriving an empirical formula that relates a parameter to an observable (see e.g. Huang et al. 2023). Additionally, it is worth noting that current efforts to implement physics-based (and other types of) models in a real-time SEP forecasting workflow via the CLEAR Space Weather Center of Excellence<sup>5</sup> are under full development (Zhao 2023).

To reduce the computational requirements, other physics-based models either assume a Parker (1958) background IMF and focus on the 3D particle transport, e.g. SPARX (Solar PArticle Radiation swX; Marsh et al. 2015), or focus on the background MHD structure and do not include particle scattering, e.g. SEPMod (Solar Energetic Particle MODel; Luhmann et al. 2007) and its recently updated versions (Palmerio et al. 2024). Within this concept, the SOLPENCO (SOLar Particle ENgineering Code; Aran et al. 2006, 2008) is based on a model that combines MHD shock simulations and particle transport simulations along single Parker field lines. It assumes that the injection of shock accelerated particles takes place at the point of the shock front magnetically connected to the observer (also known as cobpoint) (Heras et al. 1995) and then derives the evolution of the source function of shock-accelerated protons,  $Q$ , and the normalized radial velocity jump  $VR$  across the shock, at this point (Lario et al. 1998) (see Fig. 11). As a result, SOLPENCO is able to predict the flux and the cumulative fluence profiles of gradual SEP events associated with IP shocks, originating from the solar western limb to far eastern locations as seen at two heliocentric distances (Pomoell et al. 2015).

### 3.2 Multivariate Statistical and Machine Learning Methods

With the current availability of large and continually growing datasets (e.g., multi-wavelength observations from SDO, magnetograms, GOES SXR flares, SOHO/LASCO CMEs, and particle data), researchers have access to extensive resources for investigation. The relationship between parent solar events and solar energetic particles (SEPs) is complex, driven by a range of interrelated physical processes. Additionally, identifying the variables that shape the characteristics of SEP events presents a significant challenge. As a result, predictive efforts have increasingly focused on higher-dimensional correlations. This has led to the use of multivariate statistical approaches and machine learning (ML) methods (see Camporeale 2019, for a review). Such complex algorithms may potentially resolve problems that cannot be easily approached by more traditional mathematical and algorithmic tools. ML methods may provide meaningful results, under the condition that: (a) very well specified questions are put forward, and (b) a correct and consistent framework for the training and evaluation of the implemented models is formulated. Key issues for such developments include the interpretability and the reproducibility of the obtained results. ML efforts constitute one of the main pillars of modern science. For example, the number of publications in the space weather regime involving ML methods (not necessarily related to SEP forecasting) over the last decade displays an exponential growth (Fig. 12), highlighting the fact that ML complements traditional data driven (see Sect. 2) and modeling efforts (see Sect. 3).

<sup>5</sup><https://clear.ingen.umich.edu/>.

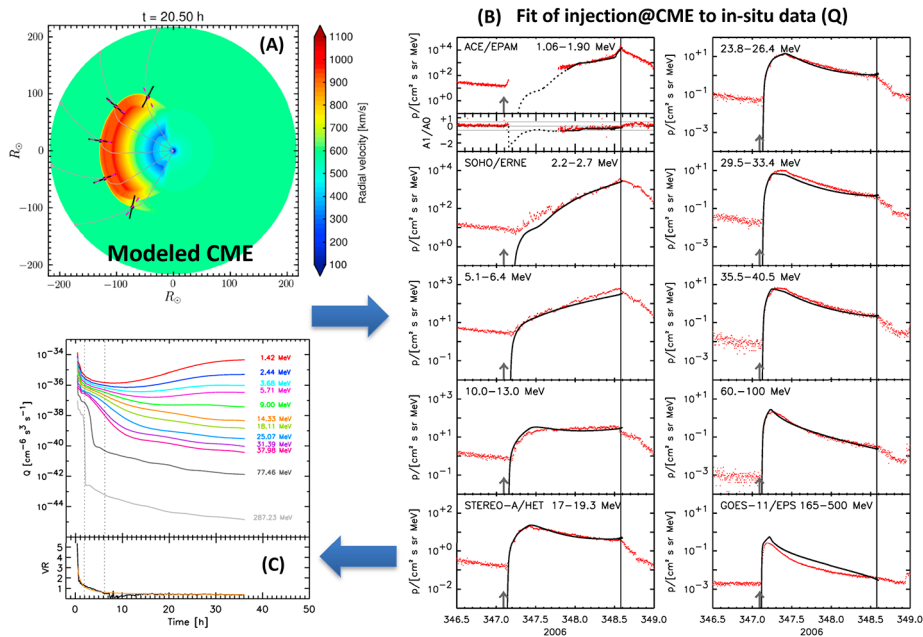
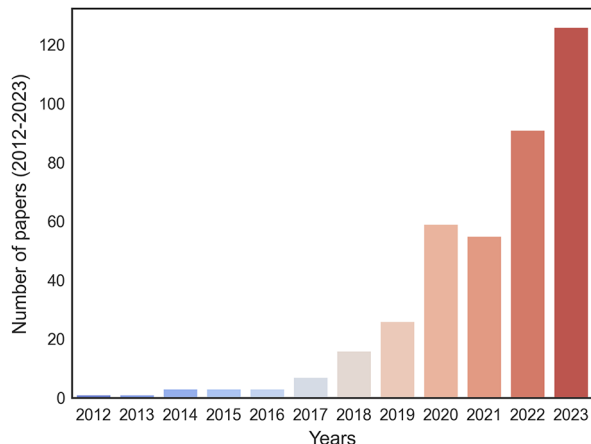


**Fig. 11** SOLPENCO outputs for the SEP even on 13 December 2006 SEP event. Panel (A): Evolution of the CME with five observers (dots) including their corresponding magnetic field lines connecting with the shock front displayed in grey. Their corresponding cobpoints are the circles on the shock front. Panel B: Simulated SEP time profiles are then compared to observations. Panel C: Since the calculated time profiles are obtained by using the evolution of the injection rate of shock-accelerated protons at the cobpoint,  $Q$ , an iterative procedure is established, aiming at identifying the optimal SEP time profile and from there the transport conditions of SEPs. Assembled from Pomoell et al. (2015)

**Fig. 12** Distribution of space weather ML published papers in referred journals from 2012–2023. Data from Web of Science (<https://www.webofscience.com/wos/woscc/basic-search>)



Space weather is among significant areas for applying ML due to the fact that on top of the continuously evolving large datasets, objectives of the predictions can be well-specified (see point (a)).

A large number of ML methods emerged in recent years that gained popularity in space weather applications (see details in Lavasa et al. 2021). Depending on the input used, such methods incorporate tabulated proxies (characteristics) of solar activity, time-series and/or images and magnetograms. One major advantage of ML methods is the possibility of extended forecasting time windows (up to a few days) that in turn allows for planning and mitigation, although these predictions have considerable uncertainty. A clear and consistent methodology should be used to check and confirm the results. This typically includes metrics such as the Probability of Detection (POD), the False Alarm Rate (FAR), the True Skill Statistic (TSS), and the Heidke Skill Score (HSS) (see the relevant metrics definitions in Jolliffe and Stephenson 2012; Lavasa et al. 2021). POD and FAR have traditionally been used by the SEP community (see e.g. Whitman et al. 2023). They both range from 0 to 100%. A perfect score for POD is 100% and for FAR is 0. Prediction methods aim at increasing POD while minimizing FAR (e.g. Balch 1999; Papaioannou et al. 2018a). HSS captures the accuracy of a prediction compared to random chance. It ranges from  $-\infty$  to 100%, with a perfect score of 100% (Heidke 1926). TSS shows how well the prediction/model can discriminate between positive and negative events. Therefore it incorporates both POD and FAR. TSS ranges from  $-100\%$  to 100%, with 100% being the perfect score and 0 indicating no skill (see also Georgoulis et al. 2024, and references therein). Additionally, direct comparisons of the obtained or predicted time-series to the observed ones are conducted to ensure accuracy and reliability. A significant remark with respect to metrics is that when evaluating models for SEP prediction, it is essential to understand the context and limitations of commonly used performance metrics. These metrics can provide valuable insights into how well a model performs on a specific dataset, but they are not universally comparable across different models, especially if the models are trained and/or evaluated under varying conditions. For example, variations in the dataset, such as differences in the time period, solar cycle phase, or instrumentation, can significantly influence the obtained metrics. Similarly, the choice of data pre-processing methods, feature engineering approaches, and evaluation metrics can introduce biases that impact the interpretation of model performance. It is, therefore, crucial to exercise caution when comparing metrics between models. Instead of relying solely on a single metric or a simple comparison, the way forward is to conduct comprehensive evaluations under controlled and consistent conditions.<sup>6</sup>

In the following, methods are divided based on their prediction windows and the applicable techniques (multivariate or ML):

- **Short-term Prediction / Nowcasting:** These methods utilize tabulated data on flares, CMEs, radio bursts, and SEP characteristics. They primarily rely on multivariate statistical methods and ML models to provide immediate forecasts, assuming that solar eruptive events have already occurred.
- **Long-term Prediction / Forecasting:** These methods either use solar images or magnetograms or time-series analysis. The initial goal is to predict the likelihood of eruptive events (such as flares and CMEs) within a predefined time window (e.g., 24 hours). The initial prediction is then extended to forecast the probability that an SEP event will accompany such an eruptive solar event.

Applicable in both forecasting and nowcasting schemes, cross-correlation techniques are employed to predict proton time-series, which have the potential to improve the accuracy and reliability of SEP forecasts over different periods (from a few hours up to a few days).

<sup>6</sup><https://ccmc.gsfc.nasa.gov/community-workshops/ccmc-sepval-2023/>.

### 3.2.1 Nowcasting - Short Term Prediction

**Multivariate Statistical Methods** Winter and Ledbetter (2015), utilized radio burst data (i.e. type II and type III radio bursts). They found that all SEP events in their sample were associated with a type II burst, and 92% were also accompanied by a type III burst. Using both the presence of these bursts and quantitative characteristics – particularly the intensity and duration of type III bursts — they applied Principal Component Analysis (PCA), together with logistic regression to make a binary (yes/no) prediction of SEP occurrence at  $E > 10$  MeV. These authors presented a POD = 65% and a FAR = 22%. PCA is a straightforward, non-parametric method of extracting relevant information from multivariable datasets and has the advantage of reducing the dimensionality of the data employed. Hence, it clears out complex datasets and highlights dependencies. Building on this, PCA and logistic regression have been successfully applied on an extensive parametric grid of both CME and flare characteristics (i.e. CME width/size and velocity, the logarithm of the SXRs flux, flare longitude, duration, and rise time) leading to a set of indices for the binary prediction of the SEP occurrence at  $E > 10$  MeV (Papaioannou et al. 2018a). In this work, the maximum POD =  $\sim 78\%$  and the relative FAR =  $\sim 41\%$ .

**Machine Learning Methods** Recently, Lavasa et al. (2021) performed a thorough analysis of different techniques to be used for the binary (i.e. yes or no) predictability of SEPs, such as logistic regression (LR), support vector machines (SVM), neural networks (NN) in the fully connected multi-layer perceptron (MLP) implementation, random forests (RF), decision trees (DTs), extremely randomized trees (ET) and extreme gradient boosting (XGB), further evaluating the importance of each solar flare (e.g. SXR flux, fluence, longitude, rise time, duration), CME (speed, width) and general (solar cycle evolution) feature employed and thus its usage in the binary (i.e. yes or no) predictability of SEPs. Moreover, feature permutation importance was used to evaluate the contribution of each input variable to the ML model. This method works by randomly shuffling (permuting) the values of a single feature and observing the resulting change in model performance. As a result, this method is used for analyzing feature contributions to a model's predictions. It is model-agnostic, meaning that it can be applied to any predictive model, regardless of its type (Rudin et al. 2022; Lavasa et al. 2021). It was concluded that the CME speed and SXR fluence are the parameters that stand out in the SEP prediction schemes applied (see Fig. 13). These authors concluded that the method of choice was RF which achieved POD =  $76 \pm 6\%$ , FAR =  $34 \pm 10\%$ , TSS =  $75 \pm 5\%$  and HSS =  $69 \pm 4\%$  in the imbalanced dataset setting. In the context of SEP prediction, the distinction between balanced and imbalanced datasets plays a critical role in model development and evaluation. A balanced dataset contains roughly equal numbers of examples for each class, positive (i.e. SEP yes) and negative (i.e. SEP no). This balance ensures that the model has ample opportunity to learn patterns for both classes, reducing the risk of bias toward the majority class. However, SEP datasets are inherently imbalanced, as SEP events are rare compared to the much more frequent negative (SEP no) scenarios (see details in Lavasa et al. 2021; Stumpo et al. 2021). In such cases, a model may either fail to capture the minority class (i.e. SEP yes), which is typically of greater interest in SEP operational context or to provide enhanced FAR (Stumpo et al. 2021). Additionally, even closer to the present time, Ali et al. (2024) applied SVM and XGB to a well-curated sample of GOES proton and SXR observations with daily resolution spanning across three solar cycles, demonstrating that XGB is the model of choice for their set-up to predict SEP events using SXR flux features. On average, the XGB (SVM) provides TSS = 72% (61%).

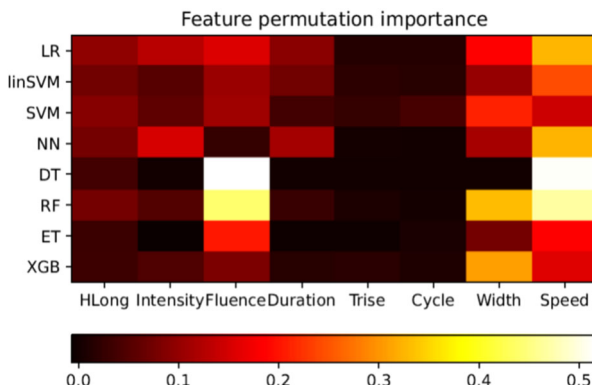


**Fig. 13** Colormap of feature permutation importance scores. The x-axis depicts the eight (8) features that were investigated, see details here above, while the y-axis presents the eight (8) ML models that were applied in the study i.e. LR, SVM, NN, RF, DT, ET and XGB (see definitions in the text). The colorbar overlays the achieved permutation importance score for each case (i.e. model & feature). The scores range from 0 to 1. In four out of eight (4/8) classifiers (i.e. LR, NN, DT, RF) the contribution of CME speed in the accomplishment of the classification task is particularly high (i.e. 0.35–0.50) labeled in yellow color. High importance scores ( $\sim 0.40$ –0.55) are also found in tree-based models (DT, RF, XGB) regarding the SXR fluence (from Lavasa et al. 2021)

Other attempts, in this direction, include the NN method that was applied to the ratio (R) of the peak SXR flux at 0.05–0.4 and 0.1–0.8 nm, aiming to the prediction of the occurrence (or not) of  $E > 10$  MeV SEP events (Kahler and Ling 2018). This is based on the work by Garcia (1994a) who demonstrated that the ratio of the two nominal bands of GOES soft X-rays can be used to compute the flare plasma temperature and emission measure. Building on this, Kahler and Ling (2018) utilized R and separated SEP events based on their achieved peak flux at an integral energy of  $E > 10$  MeV. Small SEP events were defined as those for which the  $E > 10$  MeV proton peak flux ranges between 1.2 and 10 pfu, medium sized SEP events are those with a  $E > 10$  MeV peak flux  $> 10$  pfu (i.e. NOAA criterion), and large SEP events reach  $\geq 300$  pfu. The authors found that flares that led to small SEP events were not well separated from the flares that led to non-SEPs, in contrast to  $> 10$  pfu SEP events, whereas large ( $\geq 300$  pfu) SEP events originating from flares located in the western solar hemisphere are much better separated from non-SEP flares. In a follow-up study, Ling and Kahler (2020) showed that low R values are preferentially associated with fast CMEs and SEP events at an integral energy of  $E > 10$  MeV. These authors demonstrated that the NN gives a smooth separation boundary between SEPs and non-SEPs/small SEPs, but misses some events (see also Fig. 14). However, no metrics/scores were provided. Similarly, Aminalragia-Giamini et al. (2021) presented another NN model that makes use of 26 flare related parameters revolving around the position and the SXR flux of each flare considered. They found that their model effectively predicted the large majority of SEP events investigated<sup>7</sup> and reported a mean TSS = 80% based on 100 iterations.

One category of ML SEP prediction models can be used for time-series analysis. Such models can provide predictions with windows ranging multiple hours (n-hrs) ahead. In particular, time series of SXRs and integral proton fluxes recorded by GOES were used to develop successful DT models in order to nowcast SEPs at high energies (i.e.  $E > 100$  MeV)

<sup>7</sup> SEP events were derived by the list of Pacheco Mateo (2019) who identified 257 SEPs from 1988–2013.

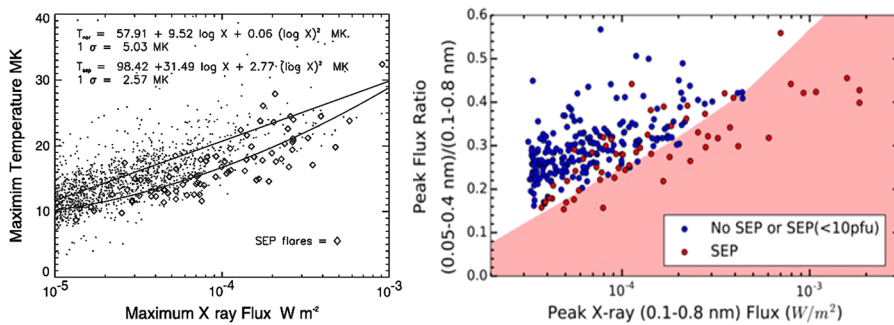


**Fig. 14** The maximum temperature (in MK) versus the maximum SXR peak flux (in  $\text{W/m}^2$ ). Flares associated to SEP events are depicted as diamonds, whereas flares not associated to SEP events as dots (from Garcia 2004; left-hand side). The Peak Flux Ratio (R) as a function of maximum SXR peak flux (in  $\text{W/m}^2$ ) for flares associated (red dots) and not associated or achieving a peak proton flux  $< 10$  pfu (blue dots) to SEP events (adapted from Kahler and Ling 2018; right-hand side)

(Boubrahimi et al. 2017). They provided a mean  $\text{POD} = 71\%$  and a  $\text{FAR} = 20\%$  (combining both of their implementations) for their balanced set-up. Most recently, in a study by the same group, data fusion models were used for the same purpose (Hosseinzadeh et al. 2024). These authors reported a  $\text{TSS} \sim 60\%$  (35%) for their balanced (imbalanced) set-up, respectively. Another recent study by Stumpo et al. (2024) used time series from SOHO/EPHIN electrons (differential electron channel E150 (0.25–0.70) MeV, E300 (0.70–3.00) MeV, E1300 (2.60–6.20) MeV, E3000 (4.80–10.40) MeV) combined with the derivative of each differential electron channel and the derivative of the proton flux. Their model predicts the logarithm of the proton flux integrated in the channels P8 (7.80–25.00 MeV), P25 (25.00–40.90 MeV), and P41 (40.90–53.00 MeV) of the EPHIN instrument. In order to do so, they created an RF model that is able to predict the energetic proton flux up to 1 hr in advance.

### 3.2.2 Forecasting (Long Term Prediction)

**Machine Learning Methods** Time series analysis has been used by Nedal et al. (2023) for the prediction of the proton integral fluxes (not only during SEP events) at  $E > 10$ ;  $E > 30$  and  $E > 60$  MeV, with forecast windows of 1,2 and 3-days in advance. This was made possible via the application of the bidirectional long short-term memory (BiLSTM) neural network model. Their model included a number of input parameters (i.e. the F10.7 index, the sunspot number, the time series of the logarithm of the SXR flux, the solar wind speed, and the average strength of the IMF) with a 1-day averaged resolution and provided the predicted proton flux. These authors provide a  $\text{POD} = 62\%$  ( $\text{FAR} = 8\%$ ) for the 1-day in advance prediction which drops (increases) when larger prediction windows are considered. Núñez and Paul-Pena (2020) have proposed a complementary approach to forecasting  $E > 10$  MeV proton events using another DT model. This method adds observations of type III radio bursts - which are used as indicators of the opening of the magnetic field lines and consequently as evidence of particles' escape into IP space (see also the ESPERTA concept described above). They obtained a  $\text{POD}$  of 70.2%, and a  $\text{FAR}$  of 40.2%.

ML-based predictions can also utilize the underlying physical connections between the accumulation, release and transformation of magnetic energy in solar eruptive events to provide an indirect approach for SEP prediction. For example, Inceoglu et al. (2018) used

the Space Weather Database Of Notification, Knowledge, Information (DONKI)<sup>8</sup> of NASA Community-Coordinated Modeling Center, to obtain their optimal results when predicting if a flare will be associated with CMEs and SEPs, resulting in  $TSS = 92(\pm 9)\%$  and  $HSS = 92(\pm 8)\%$ . Alternatively, SEPs are predicted with e.g. an BiLSTM NN, under the condition that strong flares (with a magnitude of M- or X-class) and associated CMEs are already predicted to occur, based on a model using magnetograms as input (see Abdullah et al. 2022, and references therein). For the prediction of SEPs they reported a mean (across all time windows from 12-hrs to 72 hrs ahead)  $TSS = 45.5\%$ . Similarly, ML algorithms were developed using as input magnetograms that are able to correctly disentangle cases for which an AR that produces a flare would further lead to an SEP (Kasapis et al. 2022). When utilizing the outputs from the magnetograms alone, these authors presented a mean  $TSS = 43\%$  which was further enhanced when adding to this other observational features as the flare intensity. All of these efforts, directly utilize large prediction windows (at least 12-hours and up to 72-hours in advance) that are offered, essentially, by flare and CME prediction providing context for SEP prognosis (see details in Bobra and Couvidat 2015; Bobra and Ilonidis 2016).

### 3.3 Benefits and Limitations of ML

Linkages between ML and empirical (well-established) methods provide a direct cross-comparison of results and an indirect validation of concepts. To this direction, a coherent study by Stumpo et al. (2021) compared the results of ESPERTA to a ML model and demonstrated comparable outputs in terms of metrics/scores. More importantly, this study clearly demonstrated the limitations of SEP nowcasting due to the inherent imbalance in the used samples (i.e. small size of the SEP sample as opposite to the non SEP one). Naturally, such imbalance leads to an increase in the false identifications (alarms) of a prediction system, defining a range within 25 – 45%. Their result is consistent with the results of Lavasa et al. (2021) who further demonstrated that the imbalanced setups for ML models, that are realistic and applicable to real-world problems, have—in general—false alarm rates that lie within the same range. In turn, this result highlights that models trained and tested on balanced datasets—without accounting for the natural imbalance of the problem—produce solutions that are not suitable for real-world applications, leading to challenges in transferability and reproducibility. Therefore, ML techniques are essential and can facilitate progress, but they also face the same challenges as traditional methods, imposed by the data.

## 4 Current Status

In view of the many challenges involved in SEP event prediction, there is a clear need for integrated SEP event nowcasting systems that will make use of both the current knowledge of the underlying physics in SEP events and the state-of-the-art forecast schemes already implemented. Several ensemble solutions, that incorporate different models and setups, have been developed. For example, (i) the Space Radiation Intelligence System (SPRINTS) framework which is an ensemble of expert-guided, statistical, and ML DT models (Engell et al. 2017), and (ii) the Multivariate Ensemble of Models for Probabilistic Forecast of Solar Energetic Particles (MEMPSEP) framework (Chatterjee et al. 2024) that utilizes carefully curated data (Moreland et al. 2024), coupling magnetograms to SXR time series and radio

<sup>8</sup><https://kauai.ccmc.gsfc.nasa.gov/DONKI/>.

bursts, applying a Convolution NN (CNN) approach. Both methods provide a binary classification for the SEP prediction problem. Such efforts pave the way for future attempts. Moving forward, predicting the entire SEP intensity-time profile is the next step. Towards this direction, the Advanced Solar Particle Events Casting System (ASPECS) is an automated modular advanced warning system of SEP events that couples data-driven concepts and physics-based models<sup>9</sup> (consult information within Papaioannou et al. 2022b; Whitman et al. 2023). It provides for the first time the expected SEP event time profile for a set of integral energies ( $E > 10$ -,  $> 30$ -,  $> 100$ -,  $> 300$  MeV) in near real-time mode at 1 AU. In order to do that, ASPECS incorporates many different models in sequential modules that provide predictions of: (a) SEP occurrence; (b) expected proton peak flux at respective energies of interest; (c) expected SEP time profile using a combination of simulated time profiles based on SOLPENCO2 (Aran et al. 2006; Pomoell et al. 2015) and semi-analytical solutions based on a modified Weibull fitting procedure (Kahler and Ling 2017; Paassilta et al. 2023). For (a) and (b) the Probabilistic Solar Particle Event foRecasting (PROSPER) model was developed (Papaioannou et al. 2022b). This is a Bayesian model that delivers predictions on SEP occurrence and the expected peak proton flux at 50% and 90% confidence levels (CLs). One of the advantages of ASPECS is that it provides the SEP profile time evolution, and thus it directly translates the conditions of the near Earth space into usable information during the total duration of the SEP event (see Fig. 15). In this way, such modular integrated SEP prediction systems facilitate the creation of new prediction schemes and improvement of the current (present) ones.

## 5 Future Perspectives

At present, the plans of human space exploration are in full development (Creech et al. 2022; Watson-Morgan et al. 2023). Our world is only a step away from sending humans back to the Moon and in a few years on Martian soil. Figure 16 demonstrates the importance of SEP prediction, especially concerning the associated danger to human exploration. The top panel of Fig. 16 displays the sunspot number (SSN) observed from 1995 to 2025 (blue line with units in the left vertical line) covering the solar cycles (SCs) 19 – 25. The green shaded region at the end of this period depicts the current SSN prediction of SC25 from WDC-SILSO.<sup>10</sup> We overplot, in the top panel of Fig. 16, the  $E > 30$  MeV proton omnidirectional fluence (in  $\text{cm}^{-2}$ ) of SEP events obtained by Shea and Smart (1990) (gray circles), Rotti et al. (2022a) and Papaioannou et al. (2016) (orange circles), and from calculations similar to those of Papaioannou et al. (2023) (magenta circles). The units of the  $E > 30$  MeV proton fluence are in the right vertical axis. Horizontal bars denote human spaceflight missions and/or programs of the past, present, and future. Actual measured radiation doses that were obtained during all human exploration missions (adapted from Cucinotta et al. 2008) also including estimations for a stay of 180 days at the ISS, a voyage back to the Moon and eventually to Mars, are depicted in the bottom left panel of Fig. 16. Finally, the bottom right panel of Fig. 16 displays the numerical distribution of the measured  $E > 30$  MeV proton fluences (x-axis is the logarithm of the fluence). The orange trace (right ordinate axis) provides the cumulative probability  $P(F)$  of having a  $\log(\text{fluence}) = F$  above a certain value (see also Lario and Decker 2011). The horizontal red line and the value 8.72 (indicated in red),

<sup>9</sup><https://phobos-srv.space.noa.gr/>.

<sup>10</sup><https://www.sidc.be/SILSO/forecasts>.

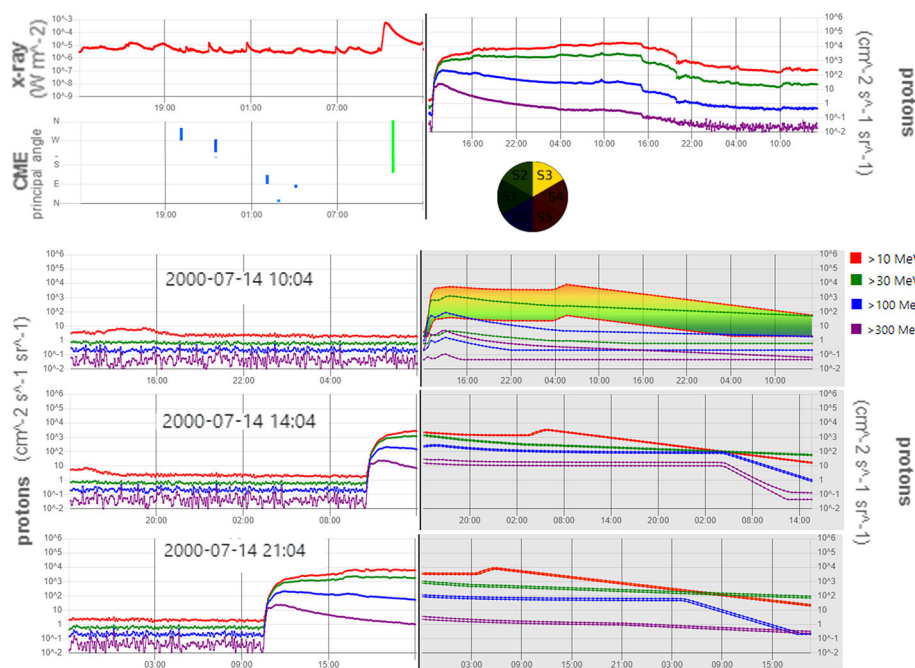


**Fig. 15** A composite output from the ASPECS tool showing the evolution of forecasts for the July 14, 2000, “Bastille Day” SEP event. On the left column, the first two top panels show the SXR flux (red line) from GOES and CMEs identified by CACTus (colored vertical lines). The top panel on the right column shows the actual measured SEP intensity profile and the pie circle the predicted solar radiation storm on the NOAA scale (<https://www.swpc.noaa.gov/noaa-space-weather-scales>) for  $E > 10$  MeV. The following three panels on the left display the proton integral fluxes at energies  $E > 10$ ,  $E > 30$ ,  $E > 100$ ,  $E > 300$  MeV measured by GOES for a period of 24 hours prior to the time indicated in each panel. That time is the time of issuing a prediction at each snapshot and separates the gray-shaded (predictions) from the white (observations) background panels at each instance. The bottom three panels on the right, with the gray background, show the predictions of the intensity time profile scaled at the 50% and 90% confidence level for each energy. The first prediction is issued at the time of the solar flare occurrence ~50 minutes prior to the arrival of the  $E > 10$  MeV particles, then the prediction constantly evolves with time and the last two panels show the obtained SEP time profiles later during the event

mark the 95% confidence level for this distribution. This means that, taking into account the complete timespan, for 5 out of 100 events, the fluence will be above this value.

Figure 16 shows that multiple SEPs have occurred during historical human space exploration. Hence it is likely that future crewed missions will also encounter strong SEP events. Moreover, since most of the missions so far lasted only a few days, the exposure of astronauts was relatively minimal (see the so-called badge dose). Once Skylab, and more importantly the space stations Mir and ISS were established, astronauts remained for longer periods of time in space and then the accumulated doses increased by almost one order of magnitude (see the biodosimetry measurements; in the bottom left panel of Fig. 16). A typical 180 day mission on the ISS leads to a 72 mSV (Cucinotta et al. 2008), denoted with a purple filled circle on the plot, reflecting the long missions that astronauts carry out presently. Today, the challenge faced by mission crews is to go beyond this limit, leaving the protection of Earth’s magnetosphere, and cope with an even higher radiation dose elevated by almost another order of magnitude – compared to what we have seen so far. This includes up to  $\sim 380$  mSv

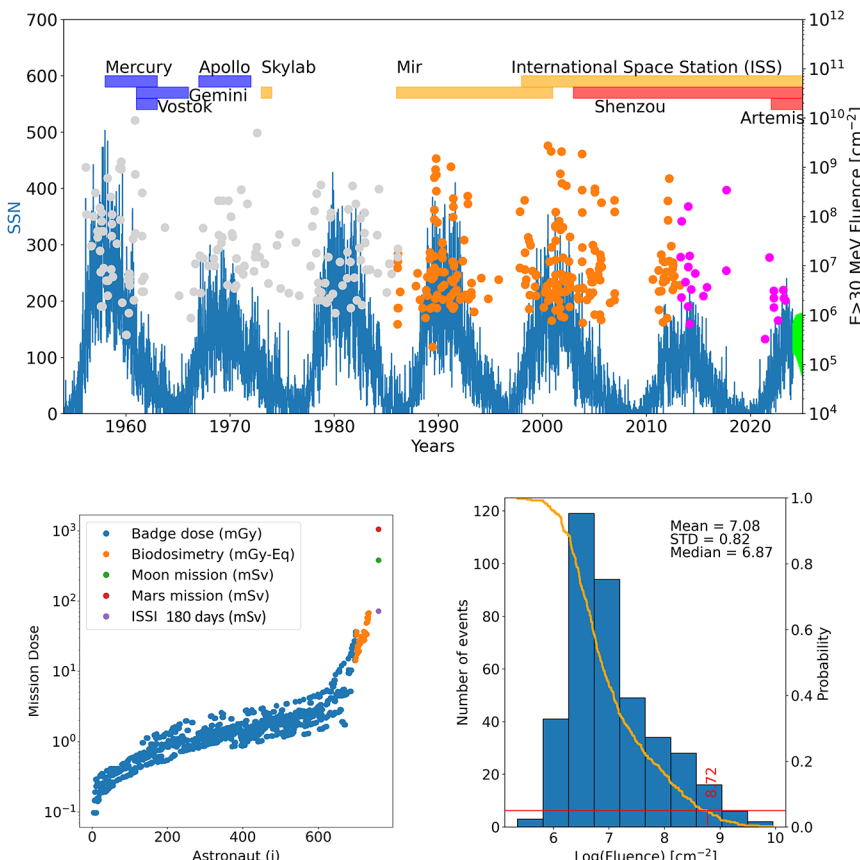


**Fig. 16** (top panel) SEP event fluence at  $E > 30$  MeV (gray, orange, and magenta circles) overlaid onto the solar cycle evolution as depicted by the sunspot number (Source: WDC-SILSO, Royal Observatory of Belgium, Brussels). SEP events were obtained by Shea and Smart (1990) (gray circles), Rotti et al. (2022a) and Papaioannou et al. (2016) (orange circles), and from calculations similar to those of Papaioannou et al. (2023) (magenta circles). (bottom panel on the left-hand side) A summary of mission personnel dosimetry from all past NASA crew (adapted from Cucinotta et al. 2008). It shows the population average Biological Dose Equivalent for astronauts on all NASA space missions, including Mercury, Gemini, Apollo, Skylab, Apollo-Soyuz, Space Shuttle, Mir and ISS missions. Estimations for a long duration mission to the ISS (72 mSv), the Moon ( $\sim 380$  mSv), and Mars ( $\sim 1050$  mSv) are also shown. (bottom panel on the right-hand side) Statistical distribution of the  $E > 30$  MeV fluences obtained using all measured SEP events reaching  $E > 30$  MeV since 1955. The orange trace (right ordinate axis) gives the probability  $P(F)$  of having a log-fluence above a certain value  $F$ . The horizontal red lines and the values indicated in red mark the 95% confidence level

for a 1 year mission on the Moon (Reitz et al. 2012) and  $\sim 1000$  mSv for a mission to Mars (Hassler et al. 2014), clearly demonstrating that humanity is on the verge of a new and significant leap into uncharted territory. Evidently, the ever-present Galactic Cosmic Ray (GCR) flux constitutes the largest radiation risk factor in such endeavors (see Liu et al. 2024, and references therein). Nonetheless, SEPs could contribute an additional radiation dose, which, in the case of the largest events, may pose a significant hazard to astronauts. The reference showcase is the 4 August 1972 SEP event (Pomerantz and Duggal 1973; Jiggens et al. 2014; Knipp et al. 2018). Apollo XVI returned to Earth on 27 April 1972, with the final Apollo XVII Moon landing was scheduled for 7 December of the same year. If the SEP event on 4

August 1972 had occurred during (such) a mission, astronauts outside the spacecraft could have faced severe radiation exposure regardless of their location (see e.g. Lockwood and Hapgood 2007).

Efficient, accurate, and timely SEP prediction incorporating the evolution of the time profile therefore becomes critical. In turn, an integrated system that mimics (but with different energies, thresholds, needs) terrestrial weather forecasting is the immediate future step (Anastasiadis et al. 2019). This latter analogy highlights similarities in the methodologies, goals, and challenges involved in both systems, in particular:

- **Timely Prediction:** Terrestrial weather forecasting seeks to predict atmospheric phenomena (e.g., storms, hurricanes) efficiently and accurately to mitigate risks. SEP prediction aims to protect space missions, humans and technology providing timely forewarning as well.
- **Evolution of Profiles:** Terrestrial weather models track the evolution of e.g. temperature, pressure, and wind profiles. Similarly, SEP prediction tools systems should account for the dynamic evolution of intensity time profiles, including variations in energy and their spatial distributions.
- **Integrated Systems:** Integrated systems that synthesize diverse data sources (from e.g. satellites and ground-based observations) into a cohesive prediction model, are needed for both the terrestrial weather and the prediction of SEPs.
- **Energy and Threshold Differences:** In terrestrial weather, thresholds for issuing warnings differ based on the type and severity of the event (e.g., a tropical storm versus a hurricane). Similarly, SEP forecasting needs to establish thresholds for different SEP energy levels and event severity to issue tailored alerts for specific users. For instance for SEPs, this would involve models for different energy levels, thresholds for hazardous conditions, and varying needs (e.g., astronaut safety versus satellite protection).

In order to accomplish this goal, the scientific community needs to:

- **Perform focused scientific work on SEP emission and transport for gradual SEP events that are directly Space Weather relevant.** In particular, the SEP transport mathematical formalism includes almost all important particle transport effects, such as particle streaming along the magnetic field, adiabatic cooling in the expanding solar wind, pitch angle and perpendicular scattering, and magnetic focusing in the diverging IMF, although, the latter is typically assumed as a Parker spiral magnetic field that does not necessarily represent the actual configuration of the perturbed interplanetary magnetic field. Enhanced modeling efforts that quantify the escaping of ions at the CME-driven shocks onto the appropriate field lines connected to the observer should be included. The obtained SEP intensity time profiles depend on (i) how the magnetic connection of the spacecraft (the observer) is established with the particle source(s), (ii) how efficiently protons are accelerated and injected by the shock into the connecting magnetic flux tube(s), (iii) how particles propagate through IP space, (iv) how the IMF irregularities modulate the SEP population and (v) how the properties of the shock are modified as it propagates through the background solar wind and large-scale solar wind structures, and (vi) how well can we describe the magnetic configuration in the inner heliosphere for each specific SEP event. Substantial progress has been made by coupling SEP transport models with MHD simulations of solar magnetic structures. Continued advancement will depend on detailed model-data comparisons, particularly for multi-spacecraft SEP events, which help constrain input parameters and improve model fidelity. Still, more work is needed to understand inter-event variations and how they reflect differences in acceleration and

transport conditions. All these factors should be further explored by using new state-of-the-art techniques, including machine learning techniques and the use of large-scale simulations of both the background solar wind medium and (coupled) SEP transport in these structures, that may have not been possible or available in the past.

- **Multi-tier Operational Systems.** The development of operational SEP forecasting systems that integrate multiple techniques is emerging as a particularly promising direction. These techniques include proxy-based methods (see Sect. 2), machine learning (ML) approaches, and physics-based SEP transport models (see Sect. 3.1). Combining these approaches into modular, multi-tiered systems enables a more effective and comprehensive use of existing capabilities (see e.g., Posner and Strauss 2020 and Sect. 4). In this context, prediction tools are becoming increasingly reliable, supported by community-wide validation efforts such as SEPVAL.<sup>11</sup> Complementary initiatives like the SEP Scoreboard<sup>12</sup> and the Integrated Solar Energetic Particle (ISEP) project<sup>13</sup> represent important early steps toward unifying observational data and diverse modeling approaches into a cohesive forecasting framework. These platforms offer real-time model outputs and enable cross-model comparisons, which are essential for improving forecast skill and supporting space missions such as Artemis and other human and robotic ventures beyond low Earth orbit. Forecasting models have shown clear improvements in accuracy, yet significant challenges remain. Predicting SEP events requires modeling a chain of complex processes—from the quiet Sun’s magnetic field, to the onset of eruptive events like flares or CMEs, to the acceleration and injection of particles, and finally, to their propagation to specific locations in the heliosphere. This end-to-end forecasting is complicated by uncertainties at each stage and by broad forecasting windows that can span from several hours to days. To address these complexities, coupling empirical data-driven techniques (e.g., proxies and ML) with physics-based models has enhanced predictive capabilities. However, a deeper understanding of the underlying physical mechanisms remains essential—particularly to support human spaceflight, where mission planning and crew safety are directly impacted, is of paramount importance to enhance the operational readiness for future space crews.
- **Long-term mission support and exploitation of observations.** Almost 70 years of intensive research into the physics, understanding, and prediction of SEP events have significantly advanced our knowledge of the key processes controlling particle acceleration, injection, and propagation throughout interplanetary space. These advances have been enabled by a succession of dedicated missions providing coordinated in situ and remote-sensing measurements of plasma, fields, particles, and electromagnetic emissions. As a result, SEP events have been observed both in and out of the ecliptic, across radial distances from  $\sim 0.3$  AU to beyond 5 AU, and at longitudinal separations spanning up to  $360^\circ$  around the Sun. A major early milestone in this effort came in the 1970s with the twin Helios spacecraft, which probed the inner heliosphere between 0.29 and 1 AU. Their observations, alongside those from near-Earth spacecraft (e.g., IMPs 7/8), widely separated observers at 1 AU, and deep-space missions like Pioneers 10/11 and Voyagers 1/2, provided foundational insights into SEP injection and transport processes (e.g., Beeck et al. 1987; Schwenn and Marsch 1990, 1991; Kunow et al. 1991; Heras et al. 1995; Reames et al. 1996; Lario et al. 2006, 2007; Strauss et al. 2017; Pacheco et al. 2019; Steyn et al.

<sup>11</sup> <https://ccmc.gsfc.nasa.gov/community-workshops/ccmc-sepval-2023/>.

<sup>12</sup> <https://ccmc.gsfc.nasa.gov/scoreboards/sep/>.

<sup>13</sup> <https://ccmc.gsfc.nasa.gov/ISEP/>.

2020; Belov et al. 2023). Importantly, multipoint measurements—even at similar heliocentric distances—have proven essential for resolving the longitudinal spread and variability of SEP events. These datasets, when fully exploited through coordinated analysis and modeling, continue to provide a critical foundation for advancing SEP forecasting. More recently, inner heliospheric missions such as Solar Orbiter (Müller et al. 2020), Parker Solar Probe (Fox et al. 2016), and BepiColombo (Benkhoff et al. 2010) have begun to fill observational gaps, offering unprecedented perspectives on SEP acceleration and transport from near the Sun out to 1 AU (e.g., Kolhöffl et al. 2021; Kouloumvakos et al. 2022; Lario et al. 2022; Papaioannou et al. 2022a; Mason et al. 2023; Rodríguez-García et al. 2023; Jebaraj et al. 2023; Mitchell et al. 2023; Raouafi et al. 2023; Kouloumvakos et al. 2024; Khoo et al. 2024; Kouloumvakos et al. 2025). These missions are modern-day explorers, traversing uncharted territories of the inner heliosphere and paving the way for our Space Odyssey. To fully exploit their observations in the context of future SEP modeling and prediction, it is essential to integrate their data into next-generation predictive frameworks that combine empirical and physics-based approaches capable of leveraging the spatial and temporal breadth of available observations. Despite these advances, several observational limitations persist. For instance, active regions producing SEP events on the far side or limbs of the Sun remain poorly observed from Earth-based vantage points. To mitigate this, missions positioned at Earth's Lagrange points L4 and L5—or even farther—are critically needed to ensure continuous, global coverage of the so-called “solar radiation hemisphere” (see Posner et al. 2021). Furthermore, reliable and sustained monitoring of high-energy protons ( $E > 300$  MeV) remains a priority, particularly given their implications for astronaut safety and spacecraft system integrity during deep space missions (see Vourlidas et al. 2023). As emphasized in Table 10 of Whitman et al. (2023), the inputs to SEP prediction models span a wide range of observations beyond particle measurements—including coronal EUV and white-light imaging, solar X-rays, radio emissions, and magnetograms. Many of these originate from research missions not designed for real-time data access or long-term continuity. Consequently, even the most advanced models are rendered ineffective when their critical inputs become unavailable. For SEP forecasting to reach true operational maturity, it is imperative that the scientific community advocate for the sustained operation of multi-domain observing assets, ensure their data are accessible in near real-time, and support the rigorous transition of validated research tools into operational environments. Only through such a comprehensive, system-level approach can we meet the growing demands of human and robotic space exploration beyond low Earth orbit.

## 6 Concluding Remarks

One of the most extraordinary accomplishments of humankind has been the ability to burst through all barriers and securely put astronauts in Earth's orbit and ultimately on the Moon. Undoubtedly, this required vision, innovation, and thorough research. As we are about to step into a Space Odyssey with human spaceflight plans reaching to the Moon and Mars the prediction of Solar Storms becomes critical. The scientific community has undertaken this challenge and will provide forewarning and thus protection to crews, with certain inherent risks, in these new ventures.

In this review, we have explored the evolution and current state of SEP forecasting, spanning empirical, physics-based, and machine learning approaches. We have highlighted the

strengths and limitations of various modeling techniques and emphasized the critical role of reliable input data and event classification standards.

As we prepare for a new era of human exploration—what we refer to as a “Space Odyssey”—accurate and timely SEP prediction is no longer optional; it is a prerequisite for mission safety. The path forward lies in integrating physical insight, robust data infrastructure, and user-focused operational models to deliver actionable forecasts. Continued collaboration across scientific, technical, and operational domains is essential for achieving this goal.

**Acknowledgements** The present work benefited from discussions held at the International Space Science Institute (ISSI, Bern, Switzerland) within the frame of the international teams: High EneRgy sOlar particle events analysis (HEROIC) [<https://www.issibern.ch/teams/heroic/>], the Role Of Solar And Stellar Energetic Particles On (Exo)Planetary Habitability (ETERNAL) [<https://www.issibern.ch/teams/exoeternal/>] and gRound and space-bAsed analySis of Strong sEp eventS and Study of their terrestrial effects (REASSESS) [<https://teams.issibern.ch/reassess/>]. The authors would like to thank both reviewers for their constructive feedback, and the thorough assessment of the manuscript. A.P. and D.L. further acknowledge support from NASA/LWS project NNH19ZDA001N-LWS. D.L. was supported by the NASA Space Weather Center of Excellence program under award No. 80NSSC23M0191 and the Heliophysics 2024 Intend Scientific Funding Model (ISFM) program. A.K. acknowledges financial support from NASA NNN06AA01C (SO-SIS Phase-E and PSP EPI-Lo) contract. This research received funding from the European Union’s Horizon Europe programme under grant agreement No 101135044 (SPEARHEAD). Views and opinions expressed are however those of the author(s) only and do not necessarily reflect those of the European Union or the European Health and Digital Executive Agency (HaDEA). Neither the European Union nor the granting authority can be held responsible for them. A.P. and R.V. are appreciative of the invitation by the organizers of European Space Weather Week (ESWW) 16 to provide a review talk on Energetic Particles in the Heliosphere. A.P. further values the invitation by the International Workshop on Machine Learning and Computer Vision in Heliophysics [[https://mosaics.astro.bas.bg/?page\\_id=165](https://mosaics.astro.bas.bg/?page_id=165)] to talk on the Prediction of Solar Activity using Machine Learning, while A.P. and A.A. are thankful for the invitation received in order to submit an article to the Ipparchos communication of the Hellenic Astronomical Society [<https://helas.gr/>] focusing on SEPs. The preparation of all the above, greatly benefited the manuscript at hand.

**Funding Information** Open access funding provided by HEAL-Link Greece.

## Declarations

**Competing Interests** The authors have no conflict of interests to declare

**Open Access** This article is licensed under a Creative Commons Attribution 4.0 International License, which permits use, sharing, adaptation, distribution and reproduction in any medium or format, as long as you give appropriate credit to the original author(s) and the source, provide a link to the Creative Commons licence, and indicate if changes were made. The images or other third party material in this article are included in the article’s Creative Commons licence, unless indicated otherwise in a credit line to the material. If material is not included in the article’s Creative Commons licence and your intended use is not permitted by statutory regulation or exceeds the permitted use, you will need to obtain permission directly from the copyright holder. To view a copy of this licence, visit <http://creativecommons.org/licenses/by/4.0/>.

## References

Abduallah Y, Jordanova VK, Liu H, Li Q, Wang JTL, Wang H (2022) Predicting solar energetic particles using SDO/HMI vector magnetic data products and a bidirectional LSTM network. *Astrophys J Suppl Ser* 260(1):16. <https://doi.org/10.3847/1538-4365/ac5f56>

Afanasiev A, Battarbee M, Vainio R (2015) Self-consistent Monte Carlo simulations of proton acceleration in coronal shocks: effect of anisotropic pitch-angle scattering of particles. *Astron Astrophys* 584:81. <https://doi.org/10.1051/0004-6361/201526750>

Afanasiev A, Vainio R, Trotta D, Nyberg S, Talebpour Sheshvan N, Hietala H, Dresing N (2023) Self-consistent modeling of the energetic storm particle event of November 10, 2012. *Astron Astrophys* 679:111. <https://doi.org/10.1051/0004-6361/202346220>

Afanasiev A, Wijsen N, Vainio R (2025) Towards advanced forecasting of solar energetic particle events with the PARASOL model. *J Space Weather Space Clim* 15:3. <https://doi.org/10.1051/swsc/2024039>

Agueda N, Klein K-L, Vilmer N, Rodríguez-Gasén R, Malandraki OE, Papaioannou A, Subirà M, Sanahuja B, Valtonen E, Dröge W, Nindos A, Heber B, Braune S, Usoskin IG, Heynderickx D, Talew E, Vainio R (2014) Release timescales of solar energetic particles in the low corona. *Astron Astrophys* 570:5. <https://doi.org/10.1051/0004-6361/201423549>

Akiyama S, Alfaro R, Alvarez C, Angeles Camacho JR, Arteaga-Velázquez JC, Arunbabu KP, Avila Rojas D, Ayala Solares HA, Belmont-Moreno E, Caballero-Mora KS, Capistrán T, Carramiñana A, Casanova S, Colin-Farias P, Cotti U, Cotzomí J, De la Fuente E, de León C, Diaz Hernandez R, Espinoza C, Fraija N, Galván-Gámez A, García D, García-González JA, Garfias F, González MM, Goodman JA, Harding JP, Hona B, Huang D, Hueyotl-Zahuantitla F, Hüntemeyer P, Iriarte A, Joshi V, Kieda D, Kunde GJ, Lara A, León Vargas H, Luis-Raya G, Malone K, Martínez-Castro J, Matthews JA, Miranda-Romagnoli P, Moreno E, Nayerhoda A, Nellen L, Newbold M, Niembro T, Nieves-Chinchilla T, Noriega-Papaqui R, Pérez-Pérez EG, Preisser L, Rho CD, Ryan J, Salazar H, Salesa Greus F, Sandoval A, Springer RW, Torres I, Ureña-Mena F, Villaseñor L, Zepeda A (2020) Interplanetary magnetic flux rope observed at ground level by HAWC. *Astrophys J* 905(1):73. <https://doi.org/10.3847/1538-4357/abc344>

Alberti T, Laurenza M, Cliver EW, Storini M, Consolini G, Lepreti F (2017) Solar activity from 2006 to 2014 and short-term forecasts of solar proton events using the ESPERTA model. *Astrophys J* 838(1):59. <https://doi.org/10.3847/1538-4357/aa5cb8>

Ali A, Sadykov V, Kosovichev A, Kitiashvili IN, Oria V, Nita GM, Illarionov E, O'Keefe PM, Francis F, Chong C-J, Kosovich P, Marroquin RD (2024) Predicting solar proton events of solar cycles 22-24 using GOES proton and soft-X-ray flux features. *Astrophys J Suppl Ser* 270(1):15. <https://doi.org/10.3847/1538-4365/ad0a6c>

Ameri D, Valtonen E, Al-Sawad A, Vainio R (2023) Relationships between energetic storm particle events and interplanetary shocks driven by full and partial halo coronal mass ejections. *Adv Space Res* 71(5):2521–2533. <https://doi.org/10.1016/j.asr.2022.12.014>

Aminalragia-Giamini S, Raptis S, Anastasiadis A, Tsigkanos A, Sandberg I, Papaioannou A, Papadimitriou C, Jiggens P, Aran A, Daglis IA (2021) Solar energetic particle event occurrence prediction using solar flare soft X-ray measurements and machine learning. *J Space Weather Space Clim* 11:59. <https://doi.org/10.1051/swsc/2021043>

Anastasiadis A, Papaioannou A, Sandberg I, Georgoulis M, Tziotziou K, Kouloumvakos A, Jiggens P (2017) Predicting flares and solar energetic particle events: the FORSPEF tool. *Sol Phys* 292(9):134. <https://doi.org/10.1007/s11207-017-1163-7>

Anastasiadis A, Lario D, Papaioannou A, Kouloumvakos A, Vourlidas A (2019) Solar energetic particles in the inner heliosphere: status and open questions. *Philos Trans R Soc Lond Ser A* 377(2148):20180100. <https://doi.org/10.1098/rsta.2018.0100>

Aran A, Sanahuja B, Lario D (2006) SOLPENCO: a solar particle engineering code. *Adv Space Res* 37(6):1240–1246. <https://doi.org/10.1016/j.asr.2005.09.019>

Aran A, Sanahuja B, Lario D (2008) Comparing proton fluxes of central meridian SEP events with those predicted by SOLPENCO. *Adv Space Res* 42(9):1492–1499. <https://doi.org/10.1016/j.asr.2007.08.003>

Bain HM, Onsager T, Mertens C, Copeland K, Benton E, Clem J, Mangeard P-S, Green J, Guild T, Tobiska W, et al (2023) Improved space weather observations and modeling for aviation radiation. *Front Astron Space Sci* 10:54. <https://doi.org/10.3389/fspas.2023.1149014>

Balch CC (1999) Sec proton prediction model: verification and analysis. *Radiat Meas* 30(3):231–250

Ball L, Melrose DB (2001) Shock drift acceleration of electrons. *Publ Astron Soc Aust* 18(4):361–373. <https://doi.org/10.1071/AS01047>

Beck MJ, Rose JM, Merkert R (2018) Exploring perceived safety, privacy, and distrust on air travel choice in the context of differing passenger screening procedures. *J Travel Res* 57(4):495–512. <https://doi.org/10.1177/0047287517700316>

Beeck J, Mason GM, Hamilton DC, Wibberenz G, Kunow H, Hovestadt D, Klecker B (1987) A multispacecraft study of the injection and transport of solar energetic particles. *Astrophys J* 322:1052. <https://doi.org/10.1086/165800>

Bell AR (1978) The acceleration of cosmic rays in shock fronts - I. *Mon Not R Astron Soc* 182:147–156. <https://doi.org/10.1093/mnras/182.2.147>

Belov A (2009) Properties of solar X-ray flares and proton event forecasting. *Adv Space Res* 43(4):467–473. <https://doi.org/10.1016/j.asr.2008.08.011>

Belov A, Garcia H, Kurt V, Mavromichalaki H, Gerontidou M (2005) Proton enhancements and their relation to the X-ray flares during the three last solar cycles. *Sol Phys* 229(1):135–159. <https://doi.org/10.1007/s11207-005-4721-3>

Belov A, Shlyk N, Abunina M, Abunin A, Papaioannou A, Richardson IG, Lario D (2023) Study of the radial dependence of Forbush decreases at 0.28–1 au using data from the Helios 1 and 2 spacecraft. *Mon Not R Astron Soc* 521(3):4652–4668. <https://doi.org/10.1093/mnras/stad732>

Benkhoff J, van Casteren J, Hayakawa H, Fujimoto M, Laakso H, Novara M, Ferri P, Middleton HR, Ziethe R (2010) BepiColombo—comprehensive exploration of Mercury: mission overview and science goals. *Planet Space Sci* 58(1–2):2–20. <https://doi.org/10.1016/j.pss.2009.09.020>

Bobra MG, Couvidat S (2015) Solar flare prediction using SDO/HMI vector magnetic field data with a machine-learning algorithm. *Astrophys J* 798(2):135. <https://doi.org/10.1088/0004-637X/798/2/135>

Bobra MG, Ilonidis S (2016) Predicting coronal mass ejections using machine learning methods. *Astrophys J* 821(2):127. <https://doi.org/10.3847/0004-637X/821/2/127>

Boubrahimi SF, Aydin B, Martens P, Angryk R (2017) On the prediction of > 100 MeV solar energetic particle events using GOES satellite data. In: 2017 IEEE international conference on big data (big data). IEEE, pp 2533–2542. <https://doi.org/10.1109/BigData.2017.8258212>

Bougeret J-L, Kaiser ML, Kellogg PJ, Manning R, Goetz K, Monson SJ, Monge N, Friel L, Meetre CA, Perche C, Sitruk L, Hoang S (1995) Waves: the Radio and Plasma Wave Investigation on the wind spacecraft. *Space Sci Rev* 71(1–4):231–263. <https://doi.org/10.1007/BF00751331>

Bougeret JL, Goetz K, Kaiser ML, Bale SD, Kellogg PJ, Maksimovic M, Monge N, Monson SJ, Astier PL, Davy S, Dekkali M, Hinze JJ, Manning RE, Aguilar-Rodriguez E, Bonnin X, Briand C, Cairns IH, Cattell CA, Cecconi B, Eastwood J, Ergun RE, Fainberg J, Hoang S, Huttunen KEJ, Krucker S, Lecacheux A, MacDowall RJ, Macher W, Mangeney A, Meetre CA, Moussas X, Nguyen QN, Oswald TH, Pulupa M, Reiner MJ, Robinson PA, Rucker H, Salem C, Santolik O, Silvis JM, Ullrich R, Zarka P, Zouganelis I (2008) S/WAVES: the Radio and Plasma Wave Investigation on the STEREO mission. *Space Sci Rev* 136(1–4):487–528. <https://doi.org/10.1007/s11214-007-9298-8>

Brüdern M, Berger L, Heber B, Heidrich-Meisner V, Klassen A, Kollhoff A, Kühl P, Strauss RD, Wimmer-Schweingruber R, Dresing N (2022) A new method to determine solar energetic particle anisotropies and their associated uncertainties demonstrated for STEREO/SEPT. *Astron Astrophys* 663:89. <https://doi.org/10.1051/0004-6361/202142761>

Bruno A, Richardson IG (2021) Empirical model of 10 - 130 MeV solar energetic particle spectra at 1 AU based on coronal mass ejection speed and direction. *Sol Phys* 296(2):36. <https://doi.org/10.1007/s11207-021-01779-4>

Bruno A, Bazilevskaya GA, Boezio M, Christian ER, de Nolfo GA, Martucci M, Merge' M, Mikhailov VV, Munini R, Richardson IG, Ryan JM, Stochaj S, Adriani O, Barbarino GC, Bellotti R, Bogomolov EA, Bongi M, Bonvicini V, Bottai S, Cafagna F, Campana D, Carlson P, Casolino M, Castellini G, De Santis C, Di Felice V, Galper AM, Karelina AV, Koldashov SV, Koldobskiy S, Krutkov SY, Kvashnin AN, Leonov A, Malakhov V, Marcelli L, Mayorov AG, Menn W, Mocchiutti E, Monaco A, Mori N, Osteria G, Panico B, Papini P, Pearce M, Picozza P, Ricci M, Ricciarini SB, Simon M, Sparvoli R, Spillantini P, Stozhkov YI, Vacchi A, Vannuccini E, Vasilyev GI, Voronov SA, Yurkin YT, Zampa G, Zampa N (2018) Solar energetic particle events observed by the PAMELA mission. *Astrophys J* 862(2):97. <https://doi.org/10.3847/1538-4357/aacc26>

Bryant DA, Cline TL, Desai UD, McDonald FB (1962) Explorer 12 observations of solar cosmic rays and energetic storm particles after the solar flare of September 28, 1961. *J Geophys Res* 67(13):4983–5000. <https://doi.org/10.1029/JZ067i013p04983>

Byrne JP (2015) Investigating the kinematics of coronal mass ejections with the automated CORIMP catalog. *J Space Weather Space Clim* 5:19. <https://doi.org/10.1051/swsc/2015020>

Camporeale E (2019) The challenge of machine learning in space weather: nowcasting and forecasting. *Space Weather* 17(8):1166–1207. <https://doi.org/10.1029/2018SW002061>

Cane HV, Stone RG (1984) Type II solar radio bursts, interplanetary shocks, and energetic particle events. *Astrophys J* 282:339–344. <https://doi.org/10.1086/162207>

Cane HV, Reames DV, von Rosenvinge TT (1988) The role of interplanetary shocks in the longitude distribution of solar energetic particles. *J Geophys Res* 93(A9):9555–9567. <https://doi.org/10.1029/JA093iA09p09555>

Cane HV, Erickson WC, Prestage NP (2002) Solar flares, type III radio bursts, coronal mass ejections, and energetic particles. *J Geophys Res Space Phys* 107(A10):1315. <https://doi.org/10.1029/2001JA000320>

Cane HV, Richardson IG, von Rosenvinge TT (2010) A study of solar energetic particle events of 1997–2006: their composition and associations. *J Geophys Res Space Phys* 115(A8):08101. <https://doi.org/10.1029/2009JA014848>

Chatterjee S, Dayeh M, Muñoz-Jaramillo A, Bain HM, Moreland K, Hart S (2024) MEMSEP-I: forecasting the probability of solar energetic particle event occurrence using a multivariate ensemble of convolutional neural networks. *Space Weather* 22:e2023SW003568. <https://doi.org/10.1029/2023SW003568>

Cliver EW, Kahler SW, Neidig DF, Cane HV, Richardson IG, Kallenrode MB, Wibberenz G (1995) Extreme “propagation” of solar energetic particles. In: International cosmic ray conference, vol 4, p 257

Cohen CMS (2006) Observations of energetic storm particles: an overview. *Geophys Monogr* 165:275–282. <https://doi.org/10.1029/165GM26>

Creech S, Guidi J, Elburn Artemis D (2022) An overview of NASA's activities to return humans to the Moon. In: 2022 IEEE Aerospace Conference (AERO). IEEE, pp 1–7. <https://doi.org/10.1109/AERO53065.2022.9843277>

Cucinotta FA, Schimmerling W, Wilson JW, Peterson LE, Badhwar GD, Saganti PB, Dicello JF (2001) Space radiation cancer risks and uncertainties for Mars missions. *Radiat Res* 156(5):682–688

Cucinotta FA, Schimmerling W, John W, Leif P, John D (2002) Space Radiation Cancer Risk Projections for Exploration Missions: Uncertainty Reduction and Mitigation. NASA technical paper (National Aeronautics and Space Administration, Lyndon B. Johnson Space Center). ISBN 9781428995581. <https://ntrs.nasa.gov/api/citations/20020073167/downloads/20020073167.pdf>

Cucinotta FA, Kim M-HY, Willingham V, George KA (2008) Physical and biological organ dosimetry analysis for International Space Station astronauts. *Radiat Res* 170(1):127–138. <https://doi.org/10.1667/RR1330.1>

Dalla S, Marsh MS, Kelly J, Laitinen T (2013) Solar energetic particle drifts in the Parker spiral. *J Geophys Res Space Phys* 118(10):5979–5985. <https://doi.org/10.1002/jgra.50589>

Desai M, Giacalone J (2016) Large gradual solar energetic particle events. *Living Rev Sol Phys* 13(1):3

Desai MI, Mason GM, Mazur JE, Dwyer JR (2006) The seed population for energetic particles accelerated by CME-driven shocks. *Space Sci Rev* 124(1–4):261–275. <https://doi.org/10.1007/s11214-006-9109-7>

Dresing N, Gómez-Herrero R, Klassen A, Heber B, Kartavykh Y, Dröge W (2012) The large longitudinal spread of solar energetic particles during the 17 January 2010 solar event. *Sol Phys* 281(1):281–300. <https://doi.org/10.1007/s11207-012-0049-y>

Dresing N, Kouloumvakos A, Vainio R, Rouillard A (2022) On the role of coronal shocks for accelerating solar energetic electrons. *Astrophys J Lett* 925(2):21. <https://doi.org/10.3847/2041-8213/ac4ca7>

Dresing N, Rodríguez-García L, Jebara IC, Warmuth A, Wallace S, Balmaceda L, Podladchikova T, Strauss RD, Kouloumvakos A, Palmroos C, Krupar V, Gieseler J, Xu Z, Mitchell JG, Cohen CMS, de Nolfo GA, Palmerio E, Carcaboso F, Kilpua EKJ, Trotta D, Auster U, Asvestari E, da Silva D, Dröge W, Getachew T, Gómez-Herrero R, Grande M, Heyner D, Holmström M, Huovelin J, Kartavykh Y, Laurenza M, Lee CO, Mason G, Maksimovic M, Mieth J, Murakami G, Oleynik P, Pinto M, Pulupa M, Richter I, Rodríguez-Pacheco J, Sánchez-Cano B, Schuller F, Ueno H, Vainio R, Vecchio A, Veronig AM, Wijsen N (2023) The 17 April 2021 widespread solar energetic particle event. *Astron Astrophys* 674:105. <https://doi.org/10.1051/0004-6361/202345938>

Dröge W, Kartavykh YY, Klecker B, Kovaltsov GA (2010) Anisotropic three-dimensional focused transport of solar energetic particles in the inner heliosphere. *Astrophys J* 709(2):912–919. <https://doi.org/10.1088/0004-637X/709/2/912>

Dröge W, Kartavykh YY, Dresing N, Heber B, Klassen A (2014) Wide longitudinal distribution of interplanetary electrons following the 7 February 2010 solar event: observations and transport modeling. *J Geophys Res Space Phys* 119(8):6074–6094. <https://doi.org/10.1002/2014JA019933>

Dröge W, Kartavykh YY, Dresing N, Klassen A (2016) Multi-spacecraft observations and transport modeling of energetic electrons for a series of solar particle events in August 2010. *Astrophys J* 826(2):134. <https://doi.org/10.3847/0004-637X/826/2/134>

Drury LO (1983) REVIEW ARTICLE: an introduction to the theory of diffusive shock acceleration of energetic particles in tenuous plasmas. *Rep Prog Phys* 46(8):973–1027. <https://doi.org/10.1088/0034-4885/46/8/002>

Eastwood JP, Lucek EA, Mazelle C, Meziane K, Narita Y, Pickett J, Treumann RA (2005) The foreshock. *Space Sci Rev* 118(1–4):41–94. <https://doi.org/10.1007/s11214-005-3824-3>

Engell AJ, Falconer DA, Schuh M, Loomis J, Bissett D (2017) SPRINTS: a framework for solar-driven event forecasting and research. *Space Weather* 15(10):1321–1346. <https://doi.org/10.1002/2017SW001660>

Falconer D, Barghouty AF, Khazanov I, Moore R (2011) A tool for empirical forecasting of major flares, coronal mass ejections, and solar particle events from a proxy of active-region free magnetic energy. *Space Weather* 9(4):04003. <https://doi.org/10.1029/2009SW000537>

Forbush SE (1946) Three unusual cosmic-ray increases possibly due to charged particles from the Sun. *Phys Rev* 70:771–772. <https://doi.org/10.1103/PhysRev.70.771>

Fox NJ, Velli MC, Bale SD, Decker R, Driesman A, Howard RA, Kasper JC, Kinnison J, Kusterer M, Lario D, Lockwood MK, McComas DJ, Raouafi NE, Szabo A (2016) The Solar Probe Plus mission: humanity's first visit to our star. *Space Sci Rev* 204(1–4):7–48. <https://doi.org/10.1007/s11214-015-0211-6>

Garcia HA (1994a) Temperature and emission measure from goes soft X-ray measurements. *Sol Phys* 154(2):275–308. <https://doi.org/10.1007/BF00681100>

Garcia HA (1994b) Temperature and hard X-ray signatures for energetic proton events. *Astrophys J* 420:422. <https://doi.org/10.1086/173572>

Garcia HA (2004) Forecasting methods for occurrence and magnitude of proton storms with solar soft X rays. *Space Weather* 2(2):02002. <https://doi.org/10.1029/2003SW000001>

Georgoulis MK, Yardley SL, Guerra JA, Murray SA, Ahmadzadeh A, Anastasiadis A, Angryk R, Aydin B, Banerjee D, Barnes G, et al (2024) Prediction of solar energetic events impacting space weather conditions. *Adv Space Res.* <https://doi.org/10.1016/j.asr.2024.02.030>

Gieseler J, Dresing N, Palmroos C, Freiherr von Forstner JL, Price DJ, Vainio R, Kouloumvakos A, Rodríguez-García L, Trotta D, Génot V, Masson A, Roth M, Veronig A (2023) Solar-MACH: an open-source tool to analyze solar magnetic connection configurations. *Front Astron Space Sci* 9:384. <https://doi.org/10.3389/fspas.2022.1058810>

Gómez-Herrero R, Dresing N, Klassen A, Heber B, Lario D, Agueda N, Malandraki OE, Blanco JJ, Rodríguez-Pacheco J, Banjac S (2015) Circumsolar energetic particle distribution on 2011 November 3. *Astrophys J* 799(1):55. <https://doi.org/10.1088/0004-637X/799/1/55>

Gopalswamy N, Yashiro S, Michalek G, Kaiser ML, Howard RA, Reames DV, Leske R, von Rosenvinge T (2002) Interacting coronal mass ejections and solar energetic particles. *Astrophys J Lett* 572(1):103–107. <https://doi.org/10.1086/341601>

Gopalswamy N, Yashiro S, Krucker S, Stenborg G, Howard RA (2004) Intensity variation of large solar energetic particle events associated with coronal mass ejections. *J Geophys Res Space Phys* 109(A12):12105. <https://doi.org/10.1029/2004JA010602>

Gosling JT (1993) The solar flare myth. *J Geophys Res* 98(A11):18937–18950. <https://doi.org/10.1029/93JA01896>

Hassler DM, Zeitlin C, Wimmer-Schweingruber RF, et al (2014) Mars' surface radiation environment measured with the Mars Science Laboratory's Curiosity rover. *Science* 343(6169):1244797. <https://doi.org/10.1126/science.1244797>

Heidke P (1926) Berechnung des erfolges und der güte der windstärkevorhersagen im sturmwarnungsdienst. *Geogr Ann* 8(4):301–349

Heras AM, Sanahuja B, Lario D, Smith ZK, Detman T, Dryer M (1995) Three low-energy particle events: modeling the influence of the parent interplanetary shock. *Astrophys J* 445:497. <https://doi.org/10.1086/175714>

Hosseinzadeh P, Filali Boubrahimi S, Hamdi SM (2024) Toward enhanced prediction of high-impact solar energetic particle events using multimodal time series data fusion models. *Space Weather* 22(6):2024-003982. <https://doi.org/10.1029/2024SW003982>

Hu J, Li G, Ao X, Zank GP, Verkhoglyadova O (2017) Modeling particle acceleration and transport at a 2-D CME-driven shock. *J Geophys Res Space Phys* 122(11):10938–10963. <https://doi.org/10.1002/2017JA024077>

Huang Z, Tóth G, Sachdeva N, Zhao L, van der Holst B, Sokolov I, Manchester WB, Gombosi TI (2023) Modeling the solar wind during different phases of the last solar cycle. *Astrophys J Lett* 946(2):47. <https://doi.org/10.3847/2041-8213/acc5ef>

Inceoglu F, Jeppesen JH, Kongstad P, Hernández Marcano NJ, Jacobsen RH, Karoff C (2018) Using machine learning methods to forecast if solar flares will be associated with CMEs and SEPs. *Astrophys J* 861(2):128. <https://doi.org/10.3847/1538-4357/aac81e>

Iucci N, Levitin AE, Belov AV, Eroshenko EA, Ptitsyna NG, Villoresi G, Chizhenkov GV, Dorman LI, Grozovska LI, Parisi M, Tyasto MI, Yanke VG (2005) Space weather conditions and spacecraft anomalies in different orbits. *Space Weather* 3(1):01001. <https://doi.org/10.1029/2003SW000056>

Jebaraj IC, Kouloumvakos A, Dresing N, Warmuth A, Wijsen N, Palmroos C, Gieseler J, Marmyleva A, Vainio R, Krupar V, Wiegelmann T, Magdalenic J, Schuller F, Battaglia AF, Fedeli A (2023) Multiple injections of energetic electrons associated with the flare and CME event on 9 October 2021. *Astron Astrophys* 675:27. <https://doi.org/10.1051/0004-6361/202245716>

Jiggens P, Chavy-Macdonald M-A, Santin G, Menicucci A, Evans H, Hilgers A (2014) The magnitude and effects of extreme solar particle events. *J Space Weather Space Clim* 4:20. <https://doi.org/10.1051/swsc/2014017>

Jolliffe IT, Stephenson DB (2012) Forecast verification: a practitioner's guide in atmospheric science. John Wiley & Sons

Kahler SW (2001) The correlation between solar energetic particle peak intensities and speeds of coronal mass ejections: effects of ambient particle intensities and energy spectra. *J Geophys Res* 106(A10):20947–20956. <https://doi.org/10.1029/2000JA002231>

Kahler SW, Ling A (2015) Dynamic SEP event probability forecasts. *Space Weather* 13(10):665–675. <https://doi.org/10.1002/2015SW001222>

Kahler SW, Ling AG (2017) Characterizing solar energetic particle event profiles with two-parameter fits. *Sol Phys* 292(4):59

Kahler SW, Ling AG (2018) Forecasting Solar Energetic Particle (SEP) events with flare X-ray peak ratios. *J Space Weather Space Clim* 8:47. <https://doi.org/10.1051/swsc/2018033>

Kahler SW, Vourlidas A (2013) A comparison of the intensities and energies of gradual solar energetic particle events with the dynamical properties of associated coronal mass ejections. *Astrophys J* 769(2):143. <https://doi.org/10.1088/0004-637X/769/2/143>

Kahler SW, Vourlidas A (2014) Do interacting coronal mass ejections play a role in solar energetic particle events? *Astrophys J* 784(1):47. <https://doi.org/10.1088/0004-637X/784/1/47>

Kahler SW, Hildner E, Van Hollebeke MAI (1978) Prompt solar proton events and coronal mass ejections. *Sol Phys* 57(2):429–443. <https://doi.org/10.1007/BF00160116>

Kahler SW, Sheeley NR Jr, Howard RA, Michels DJ, Koomen MJ, McGuire RE, von Rosenvinge TT, Reames DV (1984) Associations between coronal mass ejections and solar energetic proton events. *J Geophys Res* 89(A11):9683–9694. <https://doi.org/10.1029/JA089iA11p09683>

Kahler S, Burkepile J, Reames D (1999) Coronal/interplanetary factors contributing to the intensities of  $E > 20$  MeV gradual solar energetic particle events. In: 26th International Cosmic Ray Conference (ICRC26), vol 6, p 248

Kahler SW, Ling A, White SM (2015) Forecasting SEP events with same active region prior flares. *Space Weather* 13(2):116–123. <https://doi.org/10.1002/2014SW001099>

Kahler SW, White SM, Ling AG (2017) Forecasting  $E > 50$ -MeV proton events with the proton prediction system (PPS). *J Space Weather Space Clim* 7:27. <https://doi.org/10.1051/swsc/2017025>

Kaiser ML, Kucera TA, Davila JM, St. Cyr OC, Guhathakurta M, Christian E (2008) The STEREO mission: an introduction. *Space Sci Rev* 136(1–4):5–16. <https://doi.org/10.1007/s11214-007-9277-0>

Kallenrode M-B (1996) A statistical survey of 5-MeV proton events at transient interplanetary shocks. *J Geophys Res* 101(A11):24393–24410. <https://doi.org/10.1029/96JA01897>

Kallenrode M-B, Wibberenz G, Kunow H, Müller-Mellin R, Stolpovskii V, Kontor N (1993) Multi-spacecraft observations of particle events and interplanetary shocks during November/December 1982. *Sol Phys* 147(2):377–410. <https://doi.org/10.1007/BF00690726>

Kasapis S, Zhao L, Chen Y, Wang X, Bobra M, Gombosi T (2022) Interpretable machine learning to forecast SEP events for solar cycle 23. *Space Weather* 20(2):2021-002842. <https://doi.org/10.1029/2021SW002842>

Kelly J, Dalla S, Laitinen T (2012) Cross-field transport of solar energetic particles in a large-scale fluctuating magnetic field. *Astrophys J* 750(1):47. <https://doi.org/10.1088/0004-637X/750/1/47>

Khoo LY, Sánchez-Cano B, Lee CO, Rodríguez-García L, Kouloumvakos A, Palmerio E, Carcaboso F, Lario D, Dresing N, Cohen CMS, McComas DJ, Lynch BJ, Fraschetti F, Jebaraic IC, Mitchell JG, Nieves-Chinchilla T, Krupar V, Pacheco D, Giacalone J, Auster H-U, Benkhoff J, Bonnin X, Christian ER, Ehresmann B, Fedeli A, Fischer D, Heyner D, Holmström M, Leske RA, Maksimovic M, Mieth JZD, Oleynik P, Pinto M, Richter I, Rodríguez-Pacheco J, Schwadron NA, Schmid D, Telloni D, Vecchio A, Wiedenbeck ME (2024) Multispacecraft observations of a widespread solar energetic particle event on 2022 February 15–16. *Astrophys J* 963(2):107. <https://doi.org/10.3847/1538-4357/ad167f>

Kiplinger AL (1995) Comparative studies of hard X-ray spectral evolution in solar flares with high-energy proton events observed at Earth. *Astrophys J* 453:973. <https://doi.org/10.1086/176457>

Klein K-L (2021a) Radio astronomical tools for the study of solar energetic particles I. Correlations and diagnostics of impulsive acceleration and particle propagation. *Front Astron Space Sci* 7:105. <https://doi.org/10.3389/fspas.2020.580436>

Klein K-L (2021b) Radio astronomical tools for the study of solar energetic particles II. Time-extended acceleration at subrelativistic and relativistic energies. *Front Astron Space Sci* 7:93. <https://doi.org/10.3389/fspas.2020.580445>

Klein K-L, Dalla S (2017) Acceleration and propagation of solar energetic particles. *Space Sci Rev* 212(3–4):1107–1136. <https://doi.org/10.1007/s11214-017-0382-4>

Knipp DJ, Fraser BJ, Shea MA, Smart DF (2018) On the little-known consequences of the 4 August 1972 ultra-fast coronal mass ejection: facts, commentary, and call to action. *Space Weather* 16(11):1635–1643. <https://doi.org/10.1029/2018SW002024>

Kollhoff A, Kouloumvakos A, Lario D, Dresing N, Gómez-Herrero R, Rodríguez-García L, Malandraki OE, Richardson IG, Posner A, Klein K-L, Pacheco D, Klassen A, Heber B, Cohen CMS, Laitinen T, Cernuda I, Dalla S, Espinosa Lara F, Vainio R, Köberle M, Kühl R, Xu ZG, Berger L, Eldrum S, Brüdem M, Laurena M, Kilpua EJ, Aran A, Rouillard AP, Buřík R, Wijes N, Pomoell J, Wimmer-Schweingruber RF, Martin C, Böttcher SI, Freiherr von Forstner JL, Terasa J-C, Boden S, Kulkarni SR, Ravanbakhsh A, Yedla M, Janitzek N, Rodríguez-Pacheco J, Prieto Mateo M, Sánchez Prieto S, Parra Espada P, Rodríguez Polo O, Martínez Hellín A, Carcaboso F, Mason GM, Ho GC, Allen RC, Bruce Andrews G, Schlemm CE, Seifert H, Tyagi K, Lees WJ, Hayes J, Bale SD, Krupar V, Horbury TS, Angelini V, Evans V, O'Brien H, Maksimovic M, Khotyaintsev YV, Vecchio A, Steinvall K, Asvestari E (2021) The first widespread solar energetic particle event observed by Solar Orbiter on 2020 November 29. *Astron Astrophys* 656:20. <https://doi.org/10.1051/0004-6361/202140937>

Kouloumvakos A, Nindos A, Valtonen E, Alissandrakis CE, Malandraki O, Tsitsipis P, Kontogeorgos A, Moussas X, Hillaris A (2015) Properties of solar energetic particle events inferred from their associated radio emission. *Astron Astrophys* 580:80. <https://doi.org/10.1051/0004-6361/201424397>

Kouloumvakos A, Rouillard AP, Wu Y, Vainio R, Vourlidas A, Plotnikov I, Afanasiev A, Önel H (2019) Connecting the properties of coronal shock waves with those of solar energetic particles. *Astrophys J* 876(1):80. <https://doi.org/10.3847/1538-4357/ab15d7>

Kouloumvakos A, Kwon RY, Rodríguez-García L, Lario D, Dresing N, Kilpua EKJ, Vainio R, Török T, Plotnikov I, Rouillard AP, Downs C, Linker JA, Malandraki OE, Pinto RF, Riley P, Allen RC (2022) The first widespread solar energetic particle event of solar cycle 25 on 2020 November 29. Shock wave properties and the wide distribution of solar energetic particles. *Astron Astrophys* 660:84. <https://doi.org/10.1051/0004-6361/202142515>

Kouloumvakos A, Vainio R, Gieseler J, Price DJ (2023) The effect of shock wave properties on the release timings of solar energetic particles. *Astron Astrophys* 669:58. <https://doi.org/10.1051/0004-6361/202244363>

Kouloumvakos A, Papaioannou A, Waterfall COG, Dalla S, Vainio R, Mason GM, Heber B, Kühl P, Allen RC, Cohen CMS, Ho G, Anastasiadis A, Rouillard AP, Rodríguez-Pacheco J, Guo J, Li X, Hörlöck M, Wimmer-Schweingruber RF (2024) The multi-spacecraft high-energy solar particle event of 28 October 2021. *Astron Astrophys* 682:106. <https://doi.org/10.1051/0004-6361/202346045>

Kouloumvakos A, Wijsen N, Jebaraj IC, Afanasiev A, Lario D, Cohen CMS, Riley P, Mitchell DG, Ding Z, Vourlidas A, Giacalone J, Chen X, Hill ME (2025) Shock and SEP modeling study for the 2022 September 5 SEP event. *Astrophys J* 979(2):100. <https://doi.org/10.3847/1538-4357/ada0be>

Krymskii GF (1977) A regular mechanism for the acceleration of charged particles on the front of a shock wave. *Dokl Akad Nauk SSSR* 234:1306–1308

Kunow H, Wibberenz G, Green G, Müller-Mellin R, Kallenrode M-B (1991) Energetic particles in the inner Solar System. In: Schwenn R, Marsch E (eds) Physics of the inner heliosphere II: Particles, waves and turbulence. Springer, pp 243–342. [https://doi.org/10.1007/978-3-642-75364-0\\_6](https://doi.org/10.1007/978-3-642-75364-0_6)

Kuwabara T, Bieber JW, Clem J, Evenson P, Pyle R (2006) Development of a ground level enhancement alarm system based upon neutron monitors. *Space Weather* 4(10):10001. <https://doi.org/10.1029/2006SW000223>

Laitinen T, Dalla S, Waterfall COG, Hutchinson A (2023) Solar energetic particle event onsets at different heliolongitudes: the effect of turbulence in Parker spiral geometry. *Astron Astrophys* 673:8. <https://doi.org/10.1051/0004-6361/202346384>

Lario D, Decker RB (2002) The energetic storm particle event of October 20, 1989. *Geophys Res Lett* 29(10):1393. <https://doi.org/10.1029/2001GL014017>

Lario D, Decker RB (2011) Estimation of solar energetic proton mission-integrated fluences and peak intensities for missions traveling close to the Sun. *Space Weather* 9(11):11003. <https://doi.org/10.1029/2011SW000708>

Lario D, Karelitz A (2014) Influence of interplanetary coronal mass ejections on the peak intensity of solar energetic particle events. *J Geophys Res Space Phys* 119(6):4185–4209. <https://doi.org/10.1002/2014JA019771>

Lario D, Sanahuja B, Heras AM (1998) Energetic particle events: efficiency of interplanetary shocks as 50 keV < E < 100 MeV proton accelerators. *Astrophys J* 509(1):415–434. <https://doi.org/10.1086/306461>

Lario D, Decker RB, Roelof EC, Reisenfeld DB, Sanderson TR (2004) Low-energy particle response to CMEs during the Ulysses solar maximum northern polar passage. *J Geophys Res Space Phys* 109(A1):01107. <https://doi.org/10.1029/2003JA010071>

Lario D, Kallenrode M-B, Decker RB, Roelof EC, Krimigis SM, Aran A, Sanahuja B (2006) Radial and longitudinal dependence of solar 4–13 MeV and 27–37 MeV proton peak intensities and fluences: Helios and IMP 8 observations. *Astrophys J* 653(2):1531–1544. <https://doi.org/10.1086/508982>

Lario D, Aran A, Agueda N, Sanahuja B (2007) Radial dependence of proton peak intensities and fluences in SEP events: influence of the energetic particle transport parameters. *Adv Space Res* 40(3):289–294. <https://doi.org/10.1016/j.asr.2007.01.057>

Lario D, Aran A, Gómez-Herrero R, Dresing N, Heber B, Ho GC, Decker RB, Roelof EC (2013) Longitudinal and radial dependence of solar energetic particle peak intensities: STEREO, ACE, SOHO, GOES, and MESSENGER observations. *Astrophys J* 767(1):41. <https://doi.org/10.1088/0004-637X/767/1/41>

Lario D, Raouafi NE, Kwon R-Y, Zhang J, Gómez-Herrero R, Dresing N, Riley P (2014) The solar energetic particle event on 2013 April 11: an investigation of its solar origin and longitudinal spread. *Astrophys J* 797(1):8. <https://doi.org/10.1088/0004-637X/797/1/8>

Lario D, Kwon R-Y, Vourlidas A, Raouafi NE, Haggerty DK, Ho GC, Anderson BJ, Papaioannou A, Gómez-Herrero R, Dresing N, Riley P (2016) Longitudinal properties of a widespread solar energetic particle event on 2014 February 25: evolution of the associated CME shock. *Astrophys J* 819(1):72. <https://doi.org/10.3847/0004-637X/819/1/72>

Lario D, Kwon R-Y, Riley P, Raouafi NE (2017) On the link between the release of solar energetic particles measured at widespread heliolongitudes and the properties of the associated coronal shocks. *Astrophys J* 847(2):103. <https://doi.org/10.3847/1538-4357/aa89e3>

Lario D, Wijnen N, Kwon RY, Sánchez-Cano B, Richardson IG, Pacheco D, Palmerio E, Stevens ML, Szabo A, Heyner D, Dresing N, Gómez-Herrero R, Carcaboso F, Aran A, Afanasev A, Vainio R, Riihonen E, Poedts S, Brüden M, Xu ZG, Kollhoff A (2022) Influence of large-scale interplanetary structures on the propagation of solar energetic particles: the multispacecraft event on 2021 October 9. *Astrophys J* 934(1):55. <https://doi.org/10.3847/1538-4357/ac6efd>

Lario D, Richardson IG, Aran A, Wijnen N (2023) High-energy ( $>40$  MeV) proton intensity enhancements associated with the passage of interplanetary shocks at 1 au. *Astrophys J* 950(2):89. <https://doi.org/10.3847/1538-4357/acc9c5>

Laurenza M, Cliver EW, Hewitt J, Storini M, Ling AG, Balch CC, Kaiser ML (2009) A technique for short-term warning of solar energetic particle events based on flare location, flare size, and evidence of particle escape. *Space Weather* 7(4):04008. <https://doi.org/10.1029/2007SW000379>

Laurenza M, Alberti T, Cliver EW (2018) A short-term ESPERTA-based forecast tool for moderate-to-extreme solar proton events. *Astrophys J* 857(2):107. <https://doi.org/10.3847/1538-4357/aab712>

Laurenza M, Stumpo M, Zucca P, Mancini M, Benella S, Clark L, Alberti T, Marcucci MF (2024) Upgrades of the ESPERTA forecast tool for solar proton events. *J Space Weather Space Clim* 14:8. <https://doi.org/10.1051/swsc/2024007>

Lavasa E, Giannopoulos G, Papaioannou A, Anastasiadis A, Daglis IA, Aran A, Pacheco D, Sanahuja B (2021) Assessing the predictability of solar energetic particles with the use of machine learning techniques. *Sol Phys* 296(7):107. <https://doi.org/10.1007/s11207-021-01837-x>

Lee MA (1983) Coupled hydromagnetic wave excitation and ion acceleration at interplanetary traveling shocks. *J Geophys Res* 88(A8):6109–6120. <https://doi.org/10.1029/JA088iA08p06109>

Lee MA (2005) Coupled hydromagnetic wave excitation and ion acceleration at an evolving coronal/interplanetary shock. *Astrophys J Suppl Ser* 158(1):38–67. <https://doi.org/10.1086/428753>

Lee MA, Mewaldt RA, Giacalone J (2012) Shock acceleration of ions in the heliosphere. *Space Sci Rev* 173(1–4):247–281. <https://doi.org/10.1007/s11214-012-9932-y>

Li G, Jin M, Ding Z, Bruno A, de Nolfo GA, Randol BM, Mays L, Ryan J, Lario D (2021) Modeling the 2012 May 17 solar energetic particle event using the AWSOM and iPATH models. *Astrophys J* 919(2):146. <https://doi.org/10.3847/1538-4357/ac0db9>

Ling AG, Kahler SW (2020) Peak temperatures of large solar X-ray flares and associated CME speeds and widths. *Astrophys J* 891(1):54. <https://doi.org/10.3847/1538-4357/ab6f6c>

Linker JA, Caplan RM, Schwadron N, Gorby M, Downs C, Torok T, Lionello R, Wijaya J (2019) Coupled MHD-focused transport simulations for modeling solar particle events. *J Phys Conf Ser* 1225:012007. <https://doi.org/10.1088/1742-6596/1225/1/012007>

Liu W, Guo J, Wang Y, Slaba TC (2024) A comprehensive comparison of various galactic cosmic-ray models to the state-of-the-art particle and radiation measurements. *Astrophys J Suppl Ser* 271(1):18. <https://doi.org/10.3847/1538-4365/ad18ad>

Lockwood M, Hapgood M (2007) The rough guide to the Moon and Mars. *Astron Geophys* 48(24):6–11617. <https://doi.org/10.1111/j.1468-4004.2007.48611.x>

Luhmann JG, Ledvina SA, Krauss-Varban D, Odrstrcil D, Riley P (2007) A heliospheric simulation-based approach to SEP source and transport modeling. *Adv Space Res* 40(3):295–303. <https://doi.org/10.1016/j.asr.2007.03.089>

Marsh MS, Dalla S, Dierckxsens M, Laitinen T, Crosby NB (2015) SPARX: a modeling system for solar energetic particle radiation space weather forecasting. *Space Weather* 13(6):386–394. <https://doi.org/10.1002/2014SW001120>

Mason GM, Nitta NV, Bućk R, Gómez-Herrero R, Krupar V, Krucker S, Ho GC, Allen RC, Kouloumvakos A, Wimmer-Schweingruber RF, Rodriguez-Pacheco J, Vecchio A, Maksimovic M (2023) The 18–19 March 2022 series of  $^3\text{He}$ -rich events observed by Solar Orbiter at 0.36 au compared with EUV, X-ray, and radio observations. *Astron Astrophys* 669:16. <https://doi.org/10.1051/0004-6361/202245576>

Matthiä D, Meier MM, Berger T (2018) The solar particle event on 10–13 September 2017: spectral reconstruction and calculation of the radiation exposure in aviation and space. *Space Weather* 16(8):977–986. <https://doi.org/10.1029/2018SW001921>

Mewaldt RA, Cohen CMS, Mason GM, Cummings AC, Desai MI, Leske RA, Raines J, Stone EC, Wiedenbeck ME, von Rosenvinge TT, Zurbuchen TH (2007) On the differences in composition between solar energetic particles and solar wind. *Space Sci Rev* 130(1–4):207–219. <https://doi.org/10.1007/s11214-007-9187-1>

Mitchell JC, Cohen CMS, Eddy TJ, Joyce CJ, Rankin JS, Shen MM, de Nolfo GA, Christian ER, McCommas DJ, McNutt RL, Wiedenbeck ME, Schwadron NA, Hill ME, Labrador AW, Leske RA, Mewaldt RA, Mitchell DG, Szalay JR (2023) A living catalog of Parker Solar Probe IS $\odot$ IS energetic particle enhancements. *Astrophys J Suppl Ser* 264(2):31. <https://doi.org/10.3847/1538-4365/aca4c8>

Moreland K, Dayeh M, Bain HM, Chatterjee S, Muñoz-Jaramillo A, Hart S (2024) MEMPSEP-III. A machine learning-oriented multivariate data set for forecasting the occurrence and properties of solar energetic particle events using a multivariate ensemble approach. *Space Weather* 22:e2023SW003765. <https://doi.org/10.1029/2023SW003765>

Müller D, St. Cyr OC, Zouganelis I, Gilbert HR, Marsden R, Nieves-Chinchilla T, Antonucci E, Auchère F, Berghmans D, Horbury TS, Howard RA, Krucker S, Maksimovic M, Owen CJ, Rochus P, Rodriguez-Pacheco J, Romoli M, Solanki SK, Bruno R, Carlsson M, Fludra A, Harra L, Hassler DM, Livi S, Louarn P, Peter H, Schühle U, Teriaca L, del Toro Iniesta JC, Wimmer-Schweingruber RF, Marsch E, Velli M, De Groot A, Walsh A, Williams D (2020) The Solar Orbiter mission. *Science overview*. *Astron Astrophys* 642:1. <https://doi.org/10.1051/0004-6361/202038467>

Nedal M, Kozarev K, Arsenov N, Zhang P (2023) Forecasting solar energetic proton integral fluxes with bi-directional long short-term memory neural networks. *J Space Weather Space Clim* 13:26. <https://doi.org/10.1051/swsc/2023026>

Ng CK, Reames DV (2008) Shock acceleration of solar energetic protons: the first 10 minutes. *Astrophys J Lett* 686:123–126. <https://doi.org/10.1086/592996>

Ng CK, Reames DV, Tylka AJ (2003) Modeling shock-accelerated solar energetic particles coupled to interplanetary Alfvén waves. *Astrophys J* 591(1):461–485. <https://doi.org/10.1086/375293>

Niemela A, Wijsen N, Aran A, Rodriguez L, Magdalénic J, Poedts S (2023) Advancing interplanetary magnetohydrodynamic models through solar energetic particle modelling. *Insights from the 2013 March 15 SEP event*. *Astron Astrophys* 679:93. <https://doi.org/10.1051/0004-6361/202347116>

Núñez M (2011) Predicting solar energetic proton events ( $E > 10$  MeV). *Space Weather* 9(7):07003. <https://doi.org/10.1029/2010SW000640>

Núñez M (2015) Real-time prediction of the occurrence and intensity of the first hours of  $> 100$  MeV solar energetic proton events. *Space Weather* 13(11):807–819. <https://doi.org/10.1002/2015SW001256>

Núñez M, Paul-Pena D (2020) Predicting  $> 10$  MeV SEP events from solar flare and radio burst data. *Universe* 6(10):161. <https://doi.org/10.3390/universe6100161>

Núñez M, Reyes-Santiago PJ, Malandraki OE (2017) Real-time prediction of the occurrence of GLE events. *Space Weather* 15(7):861–873. <https://doi.org/10.1002/2017SW001605>

Nyberg S, Vuorinen L, Afanasiev A, Trotta D, Vainio R (2024) Energetic seed particles in self-consistent particle acceleration modeling at interplanetary shock waves. *Astron Astrophys.* 690:A287. <https://doi.org/10.1051/0004-6361/202451279>

Olmedo O, Zhang J, Wechsler H, Poland A, Borne K (2008) Automatic detection and tracking of coronal mass ejections in coronagraph time series. *Sol Phys* 248(2):485–499. <https://doi.org/10.1007/s11207-007-9104-5>

Owens MJ (2016) Do the legs of magnetic clouds contain twisted flux-rope magnetic fields? *Astrophys J* 818(2):197. <https://doi.org/10.3847/0004-637X/818/2/197>

Paassilta M, Raukunen O, Vainio R, Valtonen E, Papaioannou A, Siipola R, Riihonen E, Dierckxsens M, Crosby N, Malandraki O, Heber B, Klein K-L (2017) Catalogue of 55–80 MeV solar proton events extending through solar cycles 23 and 24. *J Space Weather Space Clim* 7:14. <https://doi.org/10.1051/swsc/2017013>

Paassilta M, Papaioannou A, Dresing N, Vainio R, Valtonen E, Heber B (2018) Catalogue of  $> 55$  MeV wide-longitude solar proton events observed by SOHO, ACE, and the STEREOs at  $\approx 1$  AU during 2009–2016. *Sol Phys* 293(4):70. <https://doi.org/10.1007/s11207-018-1284-7>

Paassilta M, Vainio R, Papaioannou A, Raukunen O, Barcewicz S, Anastasiadis A (2023) Magnetic connectivity and solar energetic proton event intensity profiles at deka-MeV energy. *Adv Space Res* 71(3):1840–1854. <https://doi.org/10.1016/j.asr.2022.11.051>

Pacheco Mateo D (2019) Analysis and modelling of the solar energetic particle radiation environment in the inner heliosphere in preparation for Solar Orbiter

Pacheco D, Agueda N, Aran A, Heber B, Lario D (2019) Full inversion of solar relativistic electron events measured by the Helios spacecraft. *Astron Astrophys* 624:3. <https://doi.org/10.1051/0004-6361/201834520>

Palmerio E, Luhmann JG, Mays ML, Caplan RM, Lario D, Richardson IG, Whitman K, Lee CO, Sánchez-Cano B, Wijsen N, Li Y, Cardoso C, Pinto M, Heyner D, Schmid D, Auster H-U, Fischer D (2024) Improved modelling of SEP event onset within the WSA-Enlil-SEPMOD framework. *J Space Weather Space Clim* 14:3. <https://doi.org/10.1051/swsc/2024001>

Papaioannou A (2023) What do we learn from ground level enhancements? In: NMDB@Athens: proceedings of the hybrid symposium on cosmic ray studies with neutron detectors, September 26–30, 2022, vol 2, pp 113–130. ISBN 978-3-928794-99-2. <https://doi.org/10.38072/2748-3150/p37>. [https://macau.uni-kiel.de/receive/macau\\_mods\\_00003837](https://macau.uni-kiel.de/receive/macau_mods_00003837)

Papaioannou A, Malandraki OE, Dresing N, Heber B, Klein K-L, Vainio R, Rodríguez-Gasén R, Klassen A, Nindos A, Heynderickx D, Mewaldt RA, Gómez-Herrero R, Vilmer N, Kouloumvakos A, Tziotziou K,

Tsiropoula G (2014) SEPServer catalogues of solar energetic particle events at 1 AU based on STEREO recordings: 2007–2012. *Astron Astrophys* 569:96. <https://doi.org/10.1051/0004-6361/201323336>

Papaioannou A, Sandberg I, Anastasiadis A, Kouloumvakos A, Georgoulis MK, Tziotziou K, Tsiropoula G, Jiggens P, Hilgers A (2016) Solar flares, coronal mass ejections and solar energetic particle event characteristics. *J Space Weather Space Clim* 6:42. <https://doi.org/10.1051/swsc/2016035>

Papaioannou A, Anastasiadis A, Kouloumvakos A, Paassilta M, Vainio R, Valtonen E, Belov A, Eroshenko E, Abunina M, Abunin A (2018a) Nowcasting solar energetic particle events using principal component analysis. *Sol Phys* 293(7):100. <https://doi.org/10.1007/s11207-018-1320-7>

Papaioannou A, Anastasiadis A, Sandberg I, Jiggens P (2018b) Nowcasting of solar energetic particle events using near real-time coronal mass ejection characteristics in the framework of the FORSPEF tool. *J Space Weather Space Clim* 8:37. <https://doi.org/10.1051/swsc/2018024>

Papaioannou A, Belov A, Abunina M, Eroshenko E, Abunin A, Anastasiadis A, Patsourakos S, Mavromichalaki H (2020) Interplanetary coronal mass ejections as the driver of non-recurrent Forbush decreases. *Astrophys J* 890(2):101. <https://doi.org/10.3847/1538-4357/ab6bd1>

Papaioannou A, Kouloumvakos A, Mishev A, Vainio R, Usoskin I, Herbst K, Rouillard AP, Anastasiadis A, Gieseier J, Wimmer-Schweingruber R, Kühl P (2022a) The first ground-level enhancement of solar cycle 25 on 28 October 2021. *Astron Astrophys* 660:5. <https://doi.org/10.1051/0004-6361/202142855>

Papaioannou A, Vainio R, Raukunen O, Jiggens P, Aran A, Dierckxsens M, Mallios SA, Paassilta M, Anastasiadis A (2022b) The probabilistic solar particle event forecasting (PROSPER) model. *J Space Weather Space Clim* 12:24. <https://doi.org/10.1051/swsc/2022019>

Papaioannou A, Herbst K, Ramm T, Cliver EW, Lario D, Veronig AM (2023) Revisiting empirical solar energetic particle scaling relations. I. Solar flares. *Astron Astrophys* 671:66. <https://doi.org/10.1051/0004-6361/202243407>

Papaioannou A, Vasalos G, Whitman K, Quinn P, Anastasiadis A, Mays ML, Barzolla J, Didigu C, Light C, Corti C, Jones J, Chulaki A, Hermann H, Edward S (2025) Exploring the validation results of ASPECS within ADVISOR. Solar wind

Parker EN (1958) Dynamics of the interplanetary gas and magnetic fields. *Astrophys J* 128:664. <https://doi.org/10.1086/146579>

Pomerantz MA, Duggal SP (1973) Physical sciences: record-breaking cosmic ray storm stemming from solar activity in August 1972. *Nature* 241(5388):331–333. <https://doi.org/10.1038/241331a0>

Pomoell J, Poedts S (2018) EUHFORIA: European heliospheric forecasting information asset. *J Space Weather Space Clim* 8:35. <https://doi.org/10.1051/swsc/2018020>

Pomoell J, Aran A, Jacobs C, Rodríguez-Gasén R, Poedts S, Sanahuja B (2015) Modelling large solar proton events with the shock-and-particle model. Extraction of the characteristics of the MHD shock front at the cobpoint. *J Space Weather Space Clim* 5:12. <https://doi.org/10.1051/swsc/2015015>

Posner A (2007) Up to 1-hour forecasting of radiation hazards from solar energetic ion events with relativistic electrons. *Space Weather* 5(5):05001. <https://doi.org/10.1029/2006SW000268>

Posner A, Strauss RD (2020) Warning time analysis from SEP simulations of a two-tier REleASE system applied to Mars exploration. *Space Weather* 18(4):02354. <https://doi.org/10.1029/2019SW002354>

Posner A, Arge CN, Staub J, St. Cyr OC, Folta D, Solanki SK, Strauss RDT, Effenberger F, Gandorfer A, Heber B, Henney CJ, Hirzberger J, Jones SI, Kühl P, Malandraki O, Sterken VJ (2021) A multi-purpose heliophysics L4 mission. *Space Weather* 19(9):02777. <https://doi.org/10.1029/2021SW002777>

Posner A, Malandraki OE, Karavolos M, Tziotziou K, Smanis F, Heber B, Dröge H, Kühl P, Veldes GP (2024) HESPERIA REleASE+: improving solar proton event forecasting by means of automated recognition of type-III radio bursts. *Space Weather* 22(12):2024-004013. <https://doi.org/10.1029/2024SW00401310.22541/essoar.171926580.08698491/v1>

Prinsloo PL, Strauss RD, le Roux JA (2019) Acceleration of solar wind particles by traveling interplanetary shocks. *Astrophys J* 878(2):144. <https://doi.org/10.3847/1538-4357/ab211b>

Raouafi NE, Matteini L, Squire J, Badman ST, Velli M, Klein KG, Chen CHK, Matthaeus WH, Szabo A, Linton M, Allen RC, Szalay JR, Bruno R, Decker RB, Akhavan-Tafti M, Agapitov OV, Bale SD, Bandyopadhyay R, Battams K, Berčič L, Bourouaine S, Bowen TA, Cattell C, Chandran BDG, Chhiber R, Cohen CMS, D'Amicis R, Giacalone J, Hess P, Howard RA, Horbury TS, Jagarlamudi VK, Joyce CJ, Kasper JC, Kinnison J, Laker R, Liewer P, Malaspina DM, Mann I, McComas DJ, Niembro-Hernandez T, Nieves-Chinchilla T, Panasenco O, Pokorný P, Pusack A, Pulupa M, Perez JC, Riley P, Rouillard AP, Shi C, Stenborg G, Tenerani A, Verniero JL, Viall N, Vourlidas A, Wood BE, Woodham LD, Woolley T (2023) Parker Solar Probe: four years of discoveries at solar cycle minimum. *Space Sci Rev* 219(1):8. <https://doi.org/10.1007/s11214-023-00952-4>

Reames DV (1999) Particle acceleration at the Sun and in the heliosphere. *Space Sci Rev* 90:413–491. <https://doi.org/10.1023/A:1005105831781>

Reames DV (2021) Solar energetic particles. A modern primer on understanding sources, acceleration and propagation, vol 978. <https://doi.org/10.1007/978-3-030-66402-2>

Reames DV (2023) Review and outlook of solar energetic particle measurements on multispacecraft missions. *Front Astron Space Sci* 10:1254266. <https://doi.org/10.3389/fspas.2023.1254266>

Reames DV, Barbier LM, Ng CK (1996) The spatial distribution of particles accelerated by coronal mass ejection–driven shocks. *Astrophys J* 466:473. <https://doi.org/10.1086/177525>

Reitz G, Berger T, Matthiae D (2012) Radiation exposure in the Moon environment. *Planet Space Sci* 74(1):78–83. <https://doi.org/10.1016/j.pss.2012.07.014>

Richardson IG, Cane HV (1996) Particle flows observed in ejecta during solar event onsets and their implication for the magnetic field topology. *J Geophys Res* 101(A12):27521–27532. <https://doi.org/10.1029/96JA02643>

Richardson I, Cane H (2024) Near-Earth Interplanetary Coronal Mass Ejections Since January 1996. <https://doi.org/10.7910/DVN/C2MHTH>

Richardson IG, von Rosenvinge TT, Cane HV, Christian ER, Cohen CMS, Labrador AW, Leske RA, Mewaldt RA, Wiedenbeck ME, Stone EC (2014a) > 25 MeV proton events observed by the high energy telescopes on the STEREO A and B spacecraft and/or at Earth during the first ~ seven years of the STEREO mission. *Sol Phys* 289(8):3059–3107. <https://doi.org/10.1007/s11207-014-0524-8>

Richardson I, Von Rosenvinge T, Cane H, Christian E, Cohen C, Labrador A, Leske R, Mewaldt R, Wiedenbeck M, Stone E (2014b) > 25 mev proton events observed by the high energy telescopes on the stereo a and b spacecraft and/or at Earth during the first seven years of the stereo mission. In: *Coronal magnetometry*, pp 437–485. [https://doi.org/10.1007/978-1-4939-2038-9\\_27](https://doi.org/10.1007/978-1-4939-2038-9_27)

Richardson IG, von Rosenvinge TT, Cane HV (2015) The properties of solar energetic particle event-associated coronal mass ejections reported in different CME catalogs. *Sol Phys* 290(6):1741–1759. <https://doi.org/10.1007/s11207-015-0701-4>

Richardson IG, von Rosenvinge TT, Cane HV (2017) 25 MeV solar proton events in cycle 24 and previous cycles. *Adv Space Res* 60(4):755–767. <https://doi.org/10.1016/j.asr.2016.07.035>

Richardson IG, Mays ML, Thompson BJ (2018) Prediction of solar energetic particle event peak proton intensity using a simple algorithm based on CME speed and direction and observations of associated solar phenomena. *Space Weather* 16(11):1862–1881. <https://doi.org/10.1029/2018SW002032>

Robbrecht E, Berghmans D (2004) Automated recognition of coronal mass ejections (CMEs) in near-real-time data. *Astron Astrophys* 425:1097–1106. <https://doi.org/10.1051/0004-6361:20041302>

Rodríguez-García L, Gómez-Herrero R, Dresing N, Lario D, Zouganelis I, Balmaceda LA, Kouloumvakos A, Fedeli A, Espinosa Lara F, Cernuda I, Ho GC, Wimmer-Schweingruber RF, Rodríguez-Pacheco J (2023) Solar energetic electron events measured by MESSENGER and Solar Orbiter. Peak intensity and energy spectrum radial dependences: statistical analysis. *Astron Astrophys* 670:51. <https://doi.org/10.1051/0004-6361/202244553>

Rodríguez-García L, Gómez-Herrero R, Dresing N, Balmaceda LA, Palmerio E, Kouloumvakos A, Jebraj IC, Espinosa Lara F, Roco M, Palmroos C, Warmuth A, Nicolaou G, Mason GM, Guo J, Laitinen T, Cernuda I, Nieves-Chinchilla T, Fedeli A, Lee CO, Cohen CMS, Owen CJ, Ho GC, Malandraki O, Vainio R, Rodríguez-Pacheco J (2025) Solar energetic particles injected inside and outside a magnetic cloud: the widespread solar energetic particle event on 2022 January 20. *Astron Astrophys* 694:64. <https://doi.org/10.1051/0004-6361/202452158>

Rotti S, Aydin B, Georgoulis M, Martens P (2022a) GSEP Dataset. Harvard Dataverse <https://doi.org/10.7910/DVN/DZYLHK>

Rotti S, Aydin B, Georgoulis MK, Martens PC (2022b) Integrated Geostationary Solar Energetic Particle events catalog: GSEP. *Astrophys J Suppl Ser* 262(1):29. <https://doi.org/10.3847/1538-4365/ac87ac>

Rouillard AP, Sheeley NR, Tylka A, Vourlidas A, Ng CK, Rakowski C, Cohen CMS, Mewaldt RA, Mason GM, Reames D, Savani NP, St. Cyr OC, Szabo A (2012) The longitudinal properties of a solar energetic particle event investigated using modern solar imaging. *Astrophys J* 752(1):44. <https://doi.org/10.1088/0004-637X/752/1/44>

Rudin C, Chen C, Chen Z, Huang H, Semenova L, Zhong C (2022) Interpretable machine learning: fundamental principles and 10 grand challenges. *Stat Surv* 16:1–85. <https://doi.org/10.1214/21-SS133>

Ruffolo D (1995) Effect of adiabatic deceleration on the focused transport of solar cosmic rays. *Astrophys J* 442:861. <https://doi.org/10.1086/175489>

Sanahuja B, Domingo V, Wenzel K-P, Joselyn JA, Keppler E (1983) A large proton event associated with solar filament activity. *Sol Phys* 84(1–2):321–337. <https://doi.org/10.1007/BF00157465>

Sanderson TR, Reinhard R, van Nes P, Wenzel K-P, Smith EJ, Tsurutani BT (1985) Observations of 35- to 1600-keV protons and low-frequency waves upstream of interplanetary shocks. *J Geophys Res* 90(A5):3973–3980. <https://doi.org/10.1029/JA090iA05p03973>

Santa Fe Dueñas A, Ebert RW, Dayeh MA, Desai MI, Jian LK, Li G, Smith CW (2022) Dependence of energetic storm particle heavy ion peak intensities and spectra on source CME longitude and speed. *Astrophys J* 935(1):32. <https://doi.org/10.3847/1538-4357/ac73f5>

Schwenn R, Marsch E (1990) Physics of the inner heliosphere I. Large-scale phenomena. <https://doi.org/10.1007/978-3-642-75361-9>

Schwenn R, Marsch E (1991) Physics of the inner heliosphere II. Particles, waves and turbulence. <https://doi.org/10.1007/978-3-642-75364-0>

Shalchi A (2009) Nonlinear cosmic ray diffusion theories. Springer, Berlin. <https://doi.org/10.1007/978-3-642-00309-7>

Shea MA, Smart DF (1990) A summary of major solar proton events. *Sol Phys* 127(2):297–320. <https://doi.org/10.1007/BF00152170>

Shea MA, Smart DF (1996) Solar proton fluxes as a function of the observation location with respect to the parent solar activity. *Adv Space Res* 17(4–5):225–228. [https://doi.org/10.1016/0273-1177\(95\)00574-X](https://doi.org/10.1016/0273-1177(95)00574-X)

Shea MA, Smart DF (2012) Space weather and the ground-level solar proton events of the 23rd solar cycle. *Space Sci Rev* 171(1–4):161–188. <https://doi.org/10.1007/s11214-012-9923-z>

Skilling J (1975) Cosmic ray streaming I: effect of Alfvén waves on particles. *Mon Not R Astron Soc* 172:557–566

Sokolov IV, Roussev II, Gombosi TI, Lee MA, Kóta J, Forbes TG, Manchester WB, Sakai JI (2004) A new field line advection model for solar particle acceleration. *Astrophys J Lett* 616(2):171–174. <https://doi.org/10.1086/426812>

Souvatzoglou G, Papaoannou A, Mavromichalaki H, Dimitroulakos J, Sarlanis C (2014) Optimizing the real-time ground level enhancement alert system based on neutron monitor measurements: introducing GLE Alert Plus. *Space Weather* 12(11):633–649. <https://doi.org/10.1002/2014SW001102>

St. Cyr OC, Posner A, Burkepile JT (2017) Solar energetic particle warnings from a coronagraph. *Space Weather* 15(1):240–257. <https://doi.org/10.1002/2016SW001545>

Steyn R, Strauss DT, Effenberger F, Pacheco D (2020) The soft X-ray Neupert effect as a proxy for solar energetic particle injection. A proof-of-concept physics-based forecasting model. *J Space Weather Space Clim* 10:64. <https://doi.org/10.1051/swsc/2020067>

Strauss RDT, Effenberger F (2017) A hitch-hiker's guide to stochastic differential equations. Solution methods for energetic particle transport in space physics and astrophysics. *Space Sci Rev* 212(1–2):151–192. <https://doi.org/10.1007/s11214-017-0351-y>

Strauss RD, Fichtner H (2014) Cosmic ray anisotropies near the heliopause. *Astron Astrophys* 572:3. <https://doi.org/10.1051/0004-6361/201424842>

Strauss RD, le Roux JA (2019) Solar energetic particle propagation in wave turbulence and the possibility of wave generation. *Astrophys J* 872(2):125. <https://doi.org/10.3847/1538-4357/aafe02>

Strauss RDT, Dresing N, Engelbrecht NE (2017) Perpendicular diffusion of solar energetic particles: model results and implications for electrons. *Astrophys J* 837(1):43. <https://doi.org/10.3847/1538-4357/aa5df5>

Strauss RD, Dresing N, Kollhoff A, Brüderl M (2020) On the shape of SEP electron spectra: the role of interplanetary transport. *Astrophys J* 897(1):24. <https://doi.org/10.3847/1538-4357/ab91b0>

Strauss RD, Dresing N, Richardson IG, van den Berg JP, Steyn PJ (2023) On the onset delays of solar energetic electrons and protons: evidence for a common accelerator. *Astrophys J* 951(1):2. <https://doi.org/10.3847/1538-4357/acd3ef>

Stumpo M, Benella S, Laurenza M, Alberti T, Consolini G, Marcucci MF (2021) Open issues in statistical forecasting of solar proton events: a machine learning perspective. *Space Weather* 19(10):2021-002794. <https://doi.org/10.1029/2021SW002794>

Stumpo M, Laurenza M, Benella S, Marcucci MF (2024) Predicting the energetic proton flux with a machine learning regression algorithm. *Astrophys J* 975(1):8. <https://doi.org/10.3847/1538-4357/ad7734>

Swalwell B, Dalla S, Walsh RW (2017) Solar energetic particle forecasting algorithms and associated false alarms. *Sol Phys* 292(11):173. <https://doi.org/10.1007/s11207-017-1196-y>

Tan LC, Malandraki OE, Reames DV, Ng CK, Wang L, Patsou I, Papaioannou A (2013) Comparison between path lengths traveled by solar electrons and ions in ground-level enhancement events. *Astrophys J* 768(1):68. <https://doi.org/10.1088/0004-637X/768/1/68>

Tobiska WK, Atwell W, Beck P, Benton E, Copeland K, Dyer C, Gersey B, Getley I, Hands A, Holland M, Hong S, Hwang J, Jones B, Malone K, Meier MM, Mertens C, Phillips T, Ryden K, Schwadron N, Wender SA, Wilkins R, Xapsos MA (2015) Advances in atmospheric radiation measurements and modeling needed to improve air safety. *Space Weather* 13(4):202–210. <https://doi.org/10.1002/2015SW001169>

Trotta D, Pezzi O, Burgess D, Preisser L, Blanco-Cano X, Kajdic P, Hietala H, Horbury TS, Vainio R, Dresing N, Retinò A, Marcucci MF, Sorriso-Valvo L, Servidio S, Valentini F (2023) Three-dimensional modelling of the shock-turbulence interaction. *Mon Not R Astron Soc* 525(2):1856–1866. <https://doi.org/10.1093/mnras/stad2384>

Tylka AJ, Cohen CMS, Dietrich WF, Lee MA, MacLennan CG, Mewaldt RA, Ng CK, Reames DV (2005) Shock geometry, seed populations, and the origin of variable elemental composition at high energies in large gradual solar particle events. *Astrophys J* 625(1):474–495. <https://doi.org/10.1086/429384>

Vainio R (2003) On the generation of Alfvén waves by solar energetic particles. *Astron Astrophys* 406:735–740. <https://doi.org/10.1051/0004-6361:20030822>

Vainio R, Afanasiev A (2018) Particle acceleration mechanisms. In: Malandraki OE, Crosby NB (eds) Solar particle radiation storms: forecasting and analysis. *Astrophysics and Space Science Library*, vol 444, pp 45–61. [https://doi.org/10.1007/978-3-319-60051-2\\_3](https://doi.org/10.1007/978-3-319-60051-2_3)

Vainio R, Laitinen T (2008) Simulations of coronal shock acceleration in self-generated turbulence. *J Atmos Sol-Terr Phys* 70(2–4):467–474. <https://doi.org/10.1016/j.jastp.2007.08.064>

Vainio R, Laitinen T, Carlo M (2007) Simulations of coronal diffusive shock acceleration in self-generated turbulence. *Astrophys J* 658:622–630. <https://doi.org/10.1086/510284>

Vainio R, Valtonen E, Heber B, Malandraki OE, Papaioannou A, Klein K-L, Afanasiev A, Agueda N, Aurass H, Battarbee M, Braune S, Dröge W, Ganse U, Hamadache C, Heynderickx D, Huttunen-Heikinmaa K, Kiener J, Kilian P, Kopp A, Kouloumvakos A, Maisala S, Mishev A, Miteva R, Nindos A, Oittinen T, Raukunen O, Riihonen E, Rodríguez-Gasén R, Saloniemi O, Sanahuja B, Scherer R, Spanier F, Tatischeff V, Tziotziou K, Usoskin IG, Vilmer N (2013) The first SEPServer event catalogue ~68-MeV solar proton events observed at 1 AU in 1996–2010. *J Space Weather Space Clim* 3:12. <https://doi.org/10.1051/swsc/2013030>

van den Berg J, Strauss DT, Effenberger F (2020) A primer on focused solar energetic particle transport. *Space Sci Rev* 216(8):146. <https://doi.org/10.1007/s11214-020-00771-x>

van den Berg JP, Engelbrecht NE, Wijesen N, Strauss RD (2021) On the turbulent reduction of drifts for solar energetic particles. *Astrophys J* 922(2):200. <https://doi.org/10.3847/1538-4357/ac2736>

van Haarlem MP, Wise MW, Gunst AW, Heald G, McKean JP, Hessels JWT, de Bruyn AG, Nijboer R, Swinbank J, Fallows R, Brentjens M, Nelles A, Beck R, Falcke H, Fender R, Hörandel J, Koopmans LVE, Mann G, Miley G, Röttgering H, Stappers BW, Wijers RAMJ, Zaroubi S, van den Akker M, Alexov A, Anderson J, Anderson K, van Ardenne A, Arts M, Asgekar A, Avruch IM, Batejat F, Böhnen L, Bell ME, Bell MR, van Bemmel I, Bennema P, Bentum MJ, Bernardi G, Best P, Bîrzan L, Bonafede A, Boonstra A-J, Braun R, Bregman J, Breitling F, van de Brink RH, Broderick J, Broekema PC, Brouw WN, Brüggen M, Butcher HR, van Cappellen W, Ciardi B, Coenen T, Conway J, Coolen A, Corstanje A, Damstra S, Davies O, Deller AT, Dettmar R-J, van Diepen G, Dijkstra K, Donker P, Doorduin A, Dromer J, Drost M, van Duin A, Eislöffel J, van Enst J, Ferrari C, Frieswijk W, Gankema H, Garrett MA, de Gasperin F, Gerbers M, de Geus E, Grießmeier J-M, Grit T, Gruppen P, Hamaker JP, Hassall T, Hoefl M, Holties HA, Horneffer A, van der Horst A, van Houwelingen A, Huijgen A, Iacobelli M, Intema H, Jackson N, Jelic V, de Jong A, Juette E, Kant D, Karastergiou A, Koers A, Kollen H, Kondratiev VI, Kooistra E, Koopman Y, Koster A, Kuniyoshi M, Kramer M, Kuper G, Lambropoulos P, Law C, van Leeuwen J, Lemaitre J, Loose M, Maat P, Macario G, Markoff S, Masters J, McFadden RA, McKay-Bukowski D, Meijering H, Meulman H, Mevius M, Middelberg E, Millenaar R, Miller-Jones JCA, Mohan RN, Mol JD, Morawietz J, Morganti R, Mulcahy DD, Mulder E, Munk H, Nieuwenhuis L, van Nieuwpoort R, Noordam JE, Norden M, Noutsos A, Offringa AR, Olofsson H, Omar A, Orrú E, Overeem R, Paas H, Pandey-Pommier M, Pandey VN, Pizzo R, Polatidis A, Rafferty D, Rawlings S, Reich W, de Reijer J-P, Reitsma J, Renting GA, Riemsma P, Rol E, Romein JW, Roosjen J, Ruiter M, Scaife A, van der Schaaf K, Scheers B, Schellart P, Schoenmakers A, Schoonderbeek G, Serylak M, Shulevski A, Sluman J, Smirnov O, Sobey C, Spreeuw H, Steinmetz M, Sterks CGM, Stiepel H-J, Stuurwold K, Tagger M, Tang Y, Tasse C, Thomas I, Thoudam S, Toribio MC, van der Tol B, Usov O, van Veen M, van der Veen A-J, ter Veen S, Verbiest JPW, Vermeulen R, Vermaas N, Vocks C, Vogt C, de Vos M, van der Wal E, van Weeren R, Wegemann H, Weltevrede P, White S, Wijnholds SJ, Wilhelmsson T, Wucknitz O, Yatawatta S, Zarka P, Zensus A (2013) LOFAR: the Low-Frequency ARray. *Astron Astrophys* 556:2. <https://doi.org/10.1051/0004-6361/201220873>

Van Hollebeke MAI, Ma Sung LS, McDonald FB (1975) The variation of solar proton energy spectra and size distribution with heliolongitude. *Sol Phys* 41(1):189–223. <https://doi.org/10.1007/BF00152967>

Vlahos L, Anastasiadis A, Papaioannou A, Kouloumvakos A, Isliker H (2019) Sources of solar energetic particles. *Philos Trans R Soc Lond Ser A* 377(2148):20180095. <https://doi.org/10.1098/rsta.2018.0095>

Vourlidas A, Carley EP, Vilmer N (2020) Radio observations of coronal mass ejections: space weather aspects. *Front Astron Space Sci* 7:43. <https://doi.org/10.3389/fspas.2020.00043>

Vourlidas A, Turner D, Biesecker D, Coster A, Engell A, Ho G, Immel T, Keys C, Lanzerotti L, Lu G, et al (2023) The nasa space weather science and observation gap analysis. *Adv Space Res*. <https://doi.org/10.1016/j.asr.2023.06.046>

Watson-Morgan L, Hawkins L, Carpenter L, Gagliano L, Means L, Percy TK, Polsgrove T, Vermette J, Zavrel CP (2023) Landing humans and human-class cargo on the Moon and Mars. In: 2023 IEEE Aerospace Conference. IEEE, pp 1–10

Whitman K, Egeland R, Richardson IG, Allison C, Quinn P, Barzolla J, Kitashvili I, Sadykov V, Bain HM, Dierckxsens M, Mays ML, Tadesse T, Lee KT, Semones E, Luhmann JG, Núñez M, White SM, Kahler SW, Ling AG, Smart DF, Shea MA, Tenishev V, Boubrahimi SF, Aydin B, Martens P, Angryk R, Marsh

MS, Dalla S, Crosby N, Schwadron NA, Kozarev K, Gorby M, Young MA, Laurena M, Cliver EW, Al-  
berti T, Stumpo M, Benella S, Papaioannou A, Anastasiadis A, Sandberg I, Georgoulis MK, Ji A, Kemp-  
ton D, Pandey C, Li G, Hu J, Zank GP, Lavasa E, Giannopoulos G, Falconer D, Kadadi Y, Fernandes I,  
Dayeh MA, Muñoz-Jaramillo A, Chatterjee S, Moreland KD, Sokolov IV, Roussev II, Taktakishvili A,  
Effenberger F, Gombosi T, Huang Z, Zhao L, Wijsen N, Aran A, Poedts S, Kouloumvakos A, Paassilta  
M, Vainio R, Belov A, Eroshenko EA, Abunina MA, Abunin AA, Balch CC, Malandraki O, Karavolos  
M, Heber B, Labrenz J, Kühl P, Kosovichev AG, Oria V, Nita GM, Illarionov E, O'Keefe PM, Jiang  
Y, Fereira SH, Ali A, Paouris E, Aminalragia-Giamini S, Jiggens P, Jin M, Lee CO, Palmerio E, Bruno  
A, Kasapis S, Wang X, Chen Y, Sanahuja B, Lario D, Jacobs C, Strauss DT, Steyn R, van den Berg J,  
Swalwell B, Waterfall C, Nedal M, Miteva R, Dechev M, Zucca P, Engell A, Maze B, Farmer H, Kerber  
T, Barnett B, Loomis J, Grey N, Thompson BJ, Linker JA, Caplan RM, Downs C, Török T, Lionello  
R, Titov V, Zhang M, Hosseinzadeh P (2023) Review of solar energetic particle prediction models *Adv  
Space Res* 72(12):5161–5242. <https://doi.org/10.1016/j.asr.2022.08.006>

Wiedenbeck ME, Mason GM, Cohen CMS, Nitta NV, Gómez-Herrero R, Haggerty DK (2013) Observations  
of solar energetic particles from  $^3\text{He}$ -rich events over a wide range of heliographic longitude. *Astrophys  
J* 762(1):54. <https://doi.org/10.1088/0004-637X/762/1/54>

Wijsen N (2020) PARADISE: a model for energetic particle transport in the solar wind. PhD thesis,  
Katholieke University of Leuven, Belgium

Wijsen N, Aran A, Pomoell J, Poedts S (2019) Modelling three-dimensional transport of solar energetic  
protons in a corotating interaction region generated with EUHFORIA. *Astron Astrophys* 622:28. <https://doi.org/10.1051/0004-6361/201833958>

Wijsen N, Lario D, Sánchez-Cano B, Jebaraj IC, Dresing N, Richardson IG, Aran A, Kouloumvakos A, Ding  
Z, Niemela A, Palmerio E, Carcaboso F, Vainio R, Afanasiev A, Pinto M, Pacheco D, Poedts S, Heyner D  
(2023) The effect of the ambient solar wind medium on a CME-driven shock and the associated gradual  
solar energetic particle event. *Astrophys J* 950(2):172. <https://doi.org/10.3847/1538-4357/acd1ed>

Winter LM, Ledbetter K (2015) Type II and type III radio bursts and their correlation with solar energetic  
proton events. *Astrophys J* 809(1):105. <https://doi.org/10.1088/0004-637X/809/1/105>

Woerner J, Foing B, Moon Village International Support Group (2016) The “Moon village” concept and  
initiative. In: Annual meeting of the lunar exploration analysis group, p 5084, LPI Contributions 1960

Zhang M, Qin G, Rassoul H (2009) Propagation of solar energetic particles in three-dimensional interplanetary  
magnetic fields. *Astrophys J* 692(1):109–132. <https://doi.org/10.1088/0004-637X/692/1/109>

Zhang M, Cheng L, Zhang J, Riley P, Kwon RY, Lario D, Balmaceda L, Pogorelov NV (2023) A data-  
driven, physics-based transport model of solar energetic particles accelerated by coronal mass ejection  
shocks propagating through the solar coronal and heliospheric magnetic fields. *Astrophys J Suppl Ser*  
266(2):35. <https://doi.org/10.3847/1538-4365/acb8e>

Zhao L (2023) CLEAR Space Weather Center of Excellence: All-Clear Solar Energetic Particle Prediction.  
[arXiv:2310.14677](https://arxiv.org/abs/2310.14677)

Zhao L, Sokolov I, Gombosi T, Lario D, Whitman K, Huang Z, Toth G, Manchester W, van der Holst B,  
Sachdeva N, Liu W (2024) Solar wind with field lines and energetic particles (SOFIE) model: applica-  
tion to historical solar energetic particle events. *Space Weather* 22(9):2023-003729. <https://doi.org/10.1029/2023SW003729>

**Publisher's Note** Springer Nature remains neutral with regard to jurisdictional claims in published maps and  
institutional affiliations.